Journal Pre-proofs

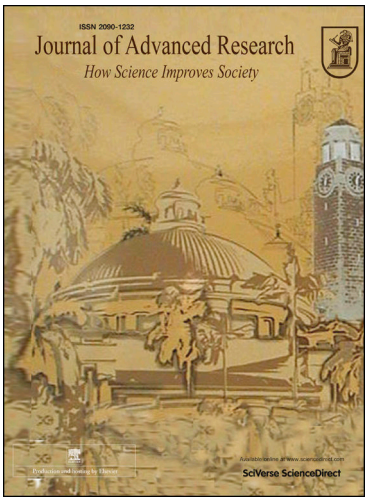

Flow-centered molecular design of vascular system breaks the trade-off between yield and appearance quality in rice

Laiyuan Zhai, Zhiyuan Zhang, Kuitian Shao, Yijun Tang, Shumila Ishfaq, Yun Wang, Kai Chen, Jianlong Xu

PII: S2090-1232(26)00392-9
DOI: https://doi.org/10.1016/j.jare.2026.05.019
Reference: JARE 2985

To appear in: *Journal of Advanced Research*

Received Date: 16 November 2025
Revised Date: 6 April 2026
Accepted Date: 6 May 2026

Please cite this article as: Zhai, L., Zhang, Z., Shao, K., Tang, Y., Ishfaq, S., Wang, Y., Chen, K., Xu, J., Flow-centered molecular design of vascular system breaks the trade-off between yield and appearance quality in rice, *Journal of Advanced Research* (2026), doi: https://doi.org/10.1016/j.jare.2026.05.019

Flow-Centered Molecular Design of Vascular System Breaks the Trade-Off Between Yield and Appearance Quality in Rice

Laiyuan Zhai[a,b,1], Zhiyuan Zhang[b,1], Kuitian Shao[c,1], Yijun Tang[e], Shumila Ishfaq[d], Yun Wang[c,*], Kai Chen[a,*], Jianlong Xu [b,a,d,*]

[a] Shenzhen Branch, Guangdong Laboratory for Lingnan Modern Agriculture, Agricultural Genomics Institute at Shenzhen, Chinese Academy of Agricultural Sciences, Shenzhen 518120, China; zhailaiyuan@caas.cn (L.Z.)

[b] State Key Laboratory of Crop Gene Resources and Breeding, Institute of Crop Sciences, Chinese Academy of Agricultural Sciences, Beijing 100081, China; kanshantea@163.com (Z.Z.)

[c] College of Agriculture, Shenyang Agricultural University, Shenyang 110866, China; 18802464027@163.com (K.S.)

[d] National Nanfan Research Institute (Sanya), Chinese Academy of Agricultural Sciences, Sanya 572024, China; 2020y90100028@caas.cn (S.I.)

[e] Department of Resources and Environment, Zunyi Normal College, Zunyi 563006, China. tangyijun1992@outlook.com (Y.T.)

[1] These authors contributed equally to this work.

* Corresponding authors: wangyun1981@syau.edu.cn (Y.W.); chenkai01@caas.cn (K.C.); xujianlong@caas.cn (J.X.)

CRediT authorship contribution statement

Laiyuan Zhai: Conceptualization, Funding acquisition, Investigation, Validation, Data curation, Formal analysis, Visualization, Writing-original draft, Writing-review & editing. **Zhiyuan Zhang:** Investigation, Visualization, Writing-review & editing. **Kuitian Shao:** Investigation, Formal analysis. **Yijun Tang**: Funding acquisition, Visualization. **Shumila Ishfaq**: Writing-review & editing. **Yun Wang**: Conceptualization, Writing-review & editing, Supervision, Data curation. **Kai Chen:** Funding acquisition, Resources, Supervision. **Jianlong Xu:** Conceptualization, Funding acquisition, Resources, Supervision, Writing-review & editing, Project administration. All authors have read and approved the published version of the manuscript.

Compliance with ethics requirement

These authors declare no conflicts of interest.

Funding

This research was supported by the National Key Research and Development Program of China (2023YFF1000400), the Shenzhen Science and Technology Program (RCBS20231211090736063), National Natural Science Foundation of China (NSFC) Young Scientists Fund (32401803), Agricultural Science and Technology Innovation Program (CAAS-ZDRW202503), and Doctoral Research Fund Project of Zunyi Normal University (No: BS[2022]12).

Data availability statement

The original contributions presented in the study are included in the

article/Supplementary data. Further inquiries can be directed to the corresponding.

Abstract:
Introduction: Achieving both high yield and superior grain quality remains a major challenge in rice breeding due to the long-standing trade-off between these traits. Enhancing vascular transport efficiency may provide a strategy to overcome this constraint, yet the genetic basis linking peduncle vascular architecture with yield-quality coordination remains poorly understood.
Objective: This study aimed to develop a flow-centered molecular design framework targeting vascular transport capacity to reconcile yield and quality in *Oryza sativa.*
Methods: Using 248 accessions from the 3K Rice Genomes panel, 14 traits related to peduncle vascular bundles, yield, and quality were phenotyped, and 31 cloned genes were haplotyped. Haplotype validity was confirmed by functional verification using near-isogenic or transgenic lines. Trait correlations, genetic effects, and pyramiding interactions of key genes were assessed. Superior haplotypes were converted into KASP markers and tested across 221 released cultivars. A breeding strategy was proposed and validated using introgression lines.
Results: The peduncle vascular bundles play a crucial role in simultaneously enhancing single-panicle weight and grain appearance quality in *japonica*/*geng* rice. Five key genes (*GL3.1*, *GW5*, *FLO2*, *LVPA4*, and *RST1*) were identified as synergistic regulators enhancing vascular development, panicle weight, and grain quality without compromising yield. A pyramiding-effect network of genes to guide the simultaneous improvement of yield and quality were constructed. Based on the uneven distribution of superior alleles among modern cultivars, a flow-centered molecular design breeding strategy was subsequently proposed and validated through the development of introgression lines, confirming that optimizing vascular systems can simultaneously improve yield and quality.
Conclusions: This study establishes a flow-centered genetic and conceptual framework linking vascular bundle architecture to yield-quality coordination and provides practical molecular tools for next-generation high-yield, high-quality rice breeding, while also offering a strategic reference for similar improvements in other crops such as wheat and maize.

Keywords: Rice molecular design breeding; yield and quality; vascular bundle in peduncle; superior haplotypes; gene pyramiding

1. Introduction

Rice (*Oryza sativa* L.) is the staple food for more than half of the world's population, making its improvement a cornerstone of global food security. Achieving the dual goal of high grain yield and superior grain quality has long been a central yet challenging objective in rice breeding. The challenge has intensified with the growing world population and rising living standards, which demand elite rice varieties that combine productivity with premium quality [1]. There is a trade-off relationship between rice yield and grain quality, primarily due to competition for assimilate

allocation during grain filling [2]. Traditional breeding strategies have primarily focused either on increasing sink capacity or improving starch quality, but few strategies have successfully reconciled the yield-quality trade-off within a single genetic framework [3]. This persistent trade-off remains a critical bottleneck, constraining the development of high-yielding, premium-quality rice varieties.

Grain yield and quality depend on the coordinated regulation of the source-flow-sink system [4,5], where grain number and size function as sinks, the upper leaves as sources, and the peduncle vascular bundle serves as the flow channel transporting photoassimilates and nutrients from source to sink. Although recent advances have improved photosynthetic efficiency in modern rice varieties (enhanced source capacity), the limited efficiency of assimilate transport and allocation of photosynthates has emerged as a major constraint on grain filling, yield, and quality enhancement [4,6]. The phloem within peduncle vascular bundles (PVB) is the principal pathway for assimilate translocation. The number of PVB is significantly positively correlated with the primary branches number (PBN) and total grain number per panicle (TGN), and the phloem area and the number of vascular bundles jointly determine nutrient transport (flow) [7,8]. In this context, "flow capacity" is defined as the efficiency and capacity of vascular tissues, particularly in panicle peduncle, in mediating assimilate transport from source to sink, which is determined by vascular bundle number, phloem area, and transport efficiency [5]. Mechanistically, vascular bundle traits influence grain quality traits such as PGWC and DEC by regulating assimilate partitioning during grain filling, as vascular bundle structure determines the efficiency of assimilate transport and distribution from source to sink [7, 9, 10]. Compared with traditional breeding strategies that primarily focus on enhancing source strength or increasing sink capacity, a flow-centered strategy emphasizes the regulatory role of assimilate transport as an intermediate layer linking source and sink. Robust stem architecture and a well-developed vascular system are the foundation for sufficient nutrient supply and for achieving high yield and good grain quality. This provides a new perspective for breaking the long-standing trade-off between grain yield and quality. However, the genetic basis of peduncle vascular bundle variation and its contribution to yield-quality coordination remain largely unexplored.

Over the past decades, only limited progress has been made in identifying genes that regulate vascular bundle development in rice. To date, a few genes such as *OsOPL1* [11], *OsCOMT* [12], *MED14_1* [13], *DVB1* [14], *LP* [15], *STRONG2* [16] and *LVPA4* [7] have been reported to regulate vascular bundle number or phloem area in panicle peduncle. In contrast, number of genes affecting the yield or quality had been cloned and well characterized, such as *GL3.1* [17], *GW5* [18], *Gn1a* [19], *sd1* [20], *IPA1* [21], *DEP1* [22], *WCR1* [23], *chalk5* [24], and *FLO2* [25]. However, the extent to which these yield- and quality-associated genes interact with PVB-related traits remains largely unexplored. With the availability of high-resolution genomic datasets such as the 3K Rice Genome Project [26], it has become feasible to systematically explore the allelic diversity in these genes and assess their combined influence on yield, quality, and vascular bundle capacity. Such integrative analysis can elucidate the role of vascular bundles in coordinating yield and quality improvement, and identify key

targets for molecular design breeding to overcome the yield-quality trade-off.

Molecular design breeding, which integrates haplotype-based gene mining, functional validation, and marker-assisted pyramiding, represents a powerful approach to combine superior alleles into elite genetic backgrounds [27]. By pyramiding superior alleles associated with the "flow" component, it may be possible to enhance assimilate transport and optimize carbohydrate partitioning, thereby achieving both high yield and superior quality. However, empirical evidence demonstrating the effective utilization of PVB-related traits and their underlying genes for coordinated improvement remains limited.

In this study, we aimed to elucidate the genetic basis of peduncle vascular bundle traits and their coordination with yield and grain quality in rice. By integrating genome-wide haplotype analysis, functional validation, and gene-interaction modeling, we established a flow-centered molecular design framework to optimize both panicle weight and grain quality. This approach identified key regulatory genes and highlighted strategies for pyramiding superior alleles, providing a foundation for next-generation high-yield and high-quality rice breeding.

2. Materials and methods

2.1. Plant materials and growth conditions

Considering the genetic diversity and the feasibility of phenotypic data investigation, a panel of 248 worldwide rice (*Oryza sativa* L.) accessions, distributed across 33 countries or regions, from the 3,000 Rice Genomes Project [26] were used in this study, including 167 *xian* (*indica*) and 81 *geng* (*japonica*) accessions (Table S1). To capture broad genetic diversity while minimizing confounding effects from population structure and developmental differences, accessions within each subspecies were selected to have relatively narrow heading date range, with 97.98% of the accessions heading between 89 and 113 days (Table S1). Field experiments were conducted at the experimental station in Sanya (18.3°N, 109.3°E), Hainan province, China during December 2015 to April 2016 and in Shenzhen city (22.5°N, 114.1°E), Guangdong province June 2016 to November 2016. Each accession was grown in three replicates, with each plot consisting of five rows of 10 plants per row, spaced 25 cm between rows and 17 cm between plants.

2.2. Measurements of the main agronomic traits used in this study

At the full heading stage, five uniform plants from the middle of each plot were selected for sampling. Stem transverse sections were excised 2 cm above the neck-panicle node and fixed in formalin–acetic–alcohol (FAA) solution. Following safranin O staining, the number of large vascular bundles (LVN), number of small vascular bundles (SVN), phloem area of large vascular bundles (LVPA, μm^2) and the phloem area of small vascular bundles (SVPA, μm^2) were quantified using an AXIO microscope (ZEISS, Germany).

For agronomic trait evaluation, eight uniform plants from the central row of each plot were sampled and oven-dried until constant weight. The following yield-related traits were recorded, including effective panicle number per plant (EPN), primary branch number (PBN), secondary branch number (SBN), total grain number per panicle (TGN), seed setting rate (SSR), thousand grain weight (TGW), grain yield per plant (GYPP, g), and single panicle weight (SPW, g). Another eight uniform plants in the middle row were harvested at maturity for measurement of grain quality related traits after air-drying, including percentage of grains with chalkiness (PGWC, %) and degree of chalkiness (DEC, %).

2.3. Haplotype analysis

To comprehensively assess genetic variation underlying key agronomic traits, a total of 31 genes were selected for this study from previously cloned and functionally validated rice genes reported to regulate key agronomic traits (Table S2), includes nine grain weight-related genes (*GS2* [28], *GS5* [29], *GL3.1* [17], *GW5* [18], *GW6* [30], *GW6a* [31], *TGW6* [32], *qTGW2* [37], and *GW2* [40]), 11 grain number per panicle (*FZP* [33], *PAY1* [34], *Gn1a* [19], *RST1* [35], *sd1* [20], *GNP1* [36], *qTGW2* [37], *IPA1* [21], *GIF1* [38], *OsSPL16* [39], *DEP1* [22]), seven vascular bundle-related genes (*OsOPL1* [11], *OsCOMT* [12], *MED14_1* [13], *DVB1* [14], *LP* [15], *STRONG2* [16] and *LVPA4* [7]), five appearance quality-related genes (*WCR1* [23], *chalk5* [24], *du3* [41], *OsAAP6* [42] and *FLO2* [25]). These genes, which are associated with grain weight, grain number per panicle, or vascular bundle number, not only regulate their respective traits but also influence grain yield. SNP genotype data for the 248 accessions were retrieved from the Rice SNP-Seek Database (http://www.oryzasnp.org/) [43]. SNPs with > 20% missing rate or minor allele frequency < 5% were filtered using PLINK [44]. Haplotype identification was performed based on non-synonymous SNPs within the coding sequences (CDS). Only major haplotypes representing >5% of the total accessions were retained for the analysis of phenotypic differences among different haplotypes. Thus, the rare haplotypes containing fewer than 12, 7 and 5 samples were excluded from the whole panel, *xian* subgroup and *geng* subgroup, respectively.

2.4. Development and evaluation of complementary transgenic lines for LVPA4

To validate the functional role of the superior *LVPA4* haplotype, complementary transgenic lines were generated using Lemont (LT; superior allele $LVPA4^{A}$) as donor and Nongken 58 (NK58; inferior allele $LVPA4^{G}$) as recipient. A 13.8-kb genomic fragment encompassing 3.4 kb upstream and 1.45 kb downstream of the LVPA4 coding sequence was amplified using KOD High-Fidelity DNA Polymerase and cloned into the binary vector pCAMBIA1300, yielding pCAMBIA1300-*LVPA4*. The recombinant construct was introduced into *Agrobacterium tumefaciens* strain EHA105 for the subsequent transformation of the *geng* variety NK58 [45]. Field experiments were conducted at the experimental station in Jiangmen city (21.3°N, 111.6°E), Guangdong

province during June to November in 2024. Each accession was grown in three replicates, with each plot consisting of ten rows of 10 plants per row, spaced 25 cm between rows and 17 cm between plants.

2.5. Development and evaluation of the near-isogenic line for RST1，GW5, GL3.1 and GW5+GL3.1

SHINCHIKU IKU 97 (SI97), carrying the inferior allele (Hap2) and the PLUS carrying the superior allele (Hap3) for *RST1*, were selected as the recipient and the donor parent, respectively. A near-isogenic line (NIL), NIL-*RST1*^{PLUS}, was developed in the SI97 background through hybridization, four backcrosses, and three selfing generations using marker-assisted selection. Similarly, using Lemont carrying the superior alleles of *GL3.1* and *GW5* as the donor parent and Teqing as the recipient parent, we constructed NILs for *GL3.1*, *GW5*, and the combination *GW5 + GL3.1* in the BC_4F_3 generation. Field experiments were conducted at the experimental station in Jiangmen city, Guangdong province during June to November in 2024. Each accession was grown in three replicates, with each plot consisting of ten rows of 10 plants per row, spaced 25 cm between rows and 17 cm between plants.

2.6. Expression patterns of important genes and their relationship

Expression patterns of five key genes (*GL3.1*, *GW5*, *FLO2*, *LVPA4* and *RST1)*, which influence vascular bundles, grain quality and SPW, were retrieved from the Rice Expression Profile Database (RiceXPro) (Version 3.0) (https://ricexpro.dna.affrc.go.jp/). The Protein-Protein Interactions (PPI) network functions enrichment analysis was performed using STRING database (Version 12.0) (https://string-db.org/) with a confidence score ≥0.7. Linkage disequilibrium (LD) between SNPs was evaluated using D’ calculated by LDBlockShow software (Version 1.40) [46].

2.7. Designing KASP markers for identifying superior alleles

Kompetitive Allele-Specific PCR (KASP) markers were designed to differentiate superior and inferior haplotypes of *GL3.1*, *GW5, FLO2*, *RST1,* and *LVPA4* based on haplotype-specific SNPs [47]. According to the identified differential SNPs, the flanking sequences were retrieved with reference to the *geng* cultivar “Nipponbare” and the *xian* cultivar “9311” to select appropriate regions for marker development. Allele-specific forward primers (each terminating with one of the SNP alleles at the 3’-end) and a common reverse primer was designed following LGC Biosearch Technologies KASP guidelines (https://www.biosearchtech.com/). The markers were validated for their accuracy in distinguishing superior alleles using fluorescence-based genotyping.

2.8. Identification of donor-derived introgressed segments

The LG31 introgression lines (IL-*RST1*^{PLUS}) were developed through hybridization followed by three rounds of backcrossing and two generations of selfing, combined with molecular marker-assisted selection. Field experiments were conducted at the experimental station in Beijing (39.5°N, 116.2°E) during May to November in 2025. Each accession was grown in three replicates, with each plot consisting of ten rows of 10 plants per row, spaced 25 cm between rows and 17 cm between plants. Whole-genome resequencing data of the recurrent parent (LG31) and the introgression line (IL-*RST1*^{PLUS}) were used to identify donor-derived genomic regions. Genomic DNA was extracted from young leaves using a standard CTAB method [48]. Whole-genome resequencing libraries were constructed following standard Illumina protocols [49], including DNA fragmentation, end repair, adapter ligation, and PCR amplification. The libraries were sequenced on an Illumina platform using a paired-end sequencing strategy. Raw reads were quality-filtered and aligned to the Nipponbare reference genome (IRGSP-1.0). SNP calling was performed using GATK [50], and high-quality SNPs were retained for further analysis. To detect putative donor-derived segments, a sliding-window approach was applied across each chromosome. Windows of 100 kb with a step size of 50 kb were scanned, and only windows containing at least 30 differential SNPs were retained for further analysis [51]. For each window, the proportion of donor alleles was calculated. Windows with donor allele proportion ≥0.9 were defined as candidate introgressed windows. Adjacent candidate windows were merged into continuous segments. The chromosome, start and end positions, number of windows, and average donor proportion for each segment were recorded. The distribution of these segments across the genome was visualized using R (v4.3.2) with the ggplot2 package.

2.9. Yeast two-hybrid assays of RST1-LVPA4, GL3.1-FLO2, and GL3.1-GW5

Yeast two-hybrid assays were performed using the GAL4 system. Full-length coding sequences were amplified from cDNA of the rice cultivar Nipponbare and cloned into the pGBKT7 (BD) and pGADT7 (AD) vectors. The constructs were co-transformed into yeast strain AH109. Transformants were selected on SD/-Leu/-Trp medium and assayed for interaction on SD/-Leu/-Trp/-His/-Ade medium.

2.10. The pyramiding effect analysis among the superior alleles

Pyramiding effects were evaluated based on effect size. Positive pyramiding effects were defined as cases where accessions carrying two superior alleles exhibited phenotypic values more than 5% higher than those carrying only one superior allele [52]. Statistical significance among groups was assessed using one-way ANOVA. The use of phenotypic gain to evaluate the effectiveness of allele combinations is consistent with previous method on haplotype-based analysis and molecular design breeding [52-54].

2.11. Statistical analysis

Statistical analysis was performed using R software (v4.3.2) and Microsoft Excel. Differences in phenotypic traits between *xian* and *geng* subgroups were examined by Student's *t*-test. Pearson's correlation coefficients among 14 traits were computed using the 'corrplot' package in R. One-way ANOVA followed by Duncan's multiple range test ($p < 0.05$) was used to evaluate phenotypic differences among gene haplotypes when more than two groups were compared. Two-tailed *t*-tests were applied for pairwise comparisons. Variance component analysis was performed using a linear mixed-effects model (LMM) to partition the phenotypic variance into genetic and environmental components. The model was fitted using the lmer function in the 'lme4' package in R.

3. Results

3.1. Test materials and phenotypic variation

The 3K RG panel represents a vast reservoir of genetic diversity and superior alleles [26]. In this study, a subset of 3K RG panel, including 167 *xian* varieties and 81 *geng* varieties, was selected based on the genetic diversity and the feasibility of phenotypic data investigation (Table S1). The 248 varieties originated from 33 countries or regions, ranging from one from Argentina, Cuba, France, Greece, Italy, Malaysia, Mexico, Peru, Solomon Islands, Spain, and Uruguay to 63 from China (Fig. 1a). Population structure and genetic relationships among accessions were characterized using genome-wide SNP data through principal component analysis (PCA) and kinship (KI) analysis (Fig. S1). Phylogenetic analysis was furtherly conducted using the Neighbor-Joining (NJ) method in MEGA (version 10) [55], based on 27,921 high-quality SNP markers divided the panel into two major clusters (Fig. 1b), a division consistent with the classification in 3K RG database (Table S1).

All phenotypic distributions of these traits were highly consistent between two years (Fig. S2a). Variance component analysis showed that genetic effects explained a substantially larger proportion of phenotypic variation than environmental effects (Fig. S2b), indicating that the traits are predominantly controlled by genotype. In addition, correlations between the two years were generally high ($p \leqslant 0.001$), suggesting stable genotypic performance across years (Fig. S2c). Therefore, we used the first-year dataset for subsequent analyses. Significant phenotypic variation was observed across all 14 measured traits in the *xian* and *geng* subgroups (Fig. 1c). Specifically, *xian* varieties exhibited significantly higher number of large vascular bundles (LVN), number of small vascular bundles (SVN), effective panicle number per plant (EPN) and grain yield per plant (GYPP) compared to *geng* varieties. Conversely, *xian* varieties had lower values for phloem area in the large vascular bundles (LVPA), small vascular bundles (SVPA), primary branch number (PBN), seed setting rate (SSR) and thousand grain weight (TGW). No significant differences were observed for five traits (percentage of grains with chalkiness (PGWC), degree of chalkiness (DEC), secondary branch number (SBN), total grain number per panicle (TGN), and single panicle weight (SPW) (Fig. 1c). These results indicate that the eight agronomic traits, including LVN, SVN, LVPA,

SVPA, PBN, SSR, EPN, and GYPP, differ significantly between *xian* and *geng* subgroups. Given the substantial phenotypic divergence between *xian* and *geng* subspecies, subsequent analyses were conducted separately within each subspecies to minimize potential confounding effects from population structure.

In *xian* subgroup, significant positive correlations were observed among LVN, LVPA, SVN and SVPA, with all of these traits showing strong positive associations with SBN, TGN and SPW. Conversely, they exhibited significant negative correlation with PGWC, DEC and EPN (Fig. 1d). No significant correlations were observed with SSR, TGW and GYPP (Fig. 1d). In contrast, the *geng* subgroup, displayed a highly significant positive correlation between LVN and LVPA. Both LVN and LVPA were significantly negatively correlated with PGWC, DEC, EPN and GYPP, while LVPA showed a significant positive correlation with SPW (Fig. 1e). Collectively, these findings suggest that vascular bundle traits play a pivotal role in determining single panicle weight (SPW) and grain appearance quality traits such as PGWC and DEC.

3.2. Haplotype analysis of 31 cloned genes in peduncle vascular bundle related traits

To explore the genetic basis of vascular bundle traits and their association with yield and quality, we conducted a haplotype analysis of 31 key genes previously linked to yield, quality, or vascular bundle traits (Table S2; Fig. 2a). Haplotype analysis revealed a variable number of haplotypes across the genes, ranging from one to eight major haplotypes. *OsSPL16* exhibited the highest haplotype diversity, with frequencies ranging from 5.24% for Hap 6, Hap7 and Hap8 to 16.9% for Hap1 in the panel (Table S3; Fig. 2b). In contrast, *GW2, qTGW6* and *IPA1* were monomorphic, thus haplotype analysis could not be used to determine their effect on vascular bundle traits. Among the remaining 28 genes, significant differences in the LVN and LVPA were observed for all except *FZP* and *du3* in the whole population. For SVN, 13 genes including *GS2*, *GS5*, *TGW6*, *RST1*, *OsSPL16*, *DEP1*, *PAY1*, *GNP1*, *FLO2*, *OsAAP6*, *LVPA4*, *DVB1* and *OsCOMT* showed significant haplotype effects. Similarly, significant differences in SVPA were observed for all multi-haplotype genes except except for *FZP*, *du3*, *STRONG2* and *LP* in whole group (Table S3; Fig. 2b).

Significant phenotypic differences were observed for the four vascular bundle-related traits (LVN, SVN, LVPA and SVPA) between *xian* and *geng* varieties (Fig. 1c). To eliminate the influence of these subspecies' differences on the vascular bundle traits, subgroup specific haplotype analysis was conducted separately for *xian* and *geng* subgroups. The number of major haplotypes in the subset ranged from one to six in the *xian* subgroup and the highest number of haplotypes was observed for *OsSPL16*, with frequency ranging from 7.78% of Hap6, Hap7 and Hap8 to 25.15% of Hap1. Significant differences in LVN, SVN, LVPA, and SVPA were detected among haplotypes of three (*GW6*, *OsAAP6* and *LP*), three (*PAY1*, *OsAAP6* and *DVB1*), six (*GS2*, *TGW6*, *DEP1*, *GNP1*, *OsAAP6* and *LP*) and four (*GS2*, *PAY1*, *GNP1* and *OsAAP6*) genes in *xian* subgroup, respectively, suggesting that these nine genes might be associated with vascular bundle traits in *xian* subgroup (Table S3; Fig. 2b).

In the *geng* subgroup, the number of major haplotypes per gene ranged from one

to five, with *GW6* showing the highest diversity (7.41% for Hap4 to 32.10% for Hap1). Significant differences in LVN, SVN, LVPA, or SVPA were observed among haplotypes of 11 genes, including *GL3.1*, *GW5*, *GW6*, *TGW6*, *RST1*, *PAY1*, *FLO2*, *LVPA4*, *STRONG2*, *DVB1* and *MED14_1* (Table S3; Fig. 2b), indicating that these genes might be related to vascular bundle traits in the *geng* subgroup.

3.3. Relationship analysis between peduncle vascular bundles, yield and quality through haplotype analysis

To elucidate the influence of these genes on yield and quality related traits, as well as their relationships with vascular bundles, haplotype analysis was conducted. Eleven genes (*GL3.1*, *GW5*, *GW6*, *TGW6*, *RST1*, *PAY1*, *FLO2*, *LVPA4*, *STRONG2*, *DVB1* and *MED14_1*) and nine genes (*OsAAP6*, *GW6*, *LP*, *PAY1*, *DVB1*, *GS2*, *GNP1*, *TGW6* and *DEP1*) were analyzed in *geng* and *xian* subgroups, respectively. The analysis included two traits related to appearance quality (PGWC and DEC) and eight traits associated with grain yield (TGW, PBN, SBN, TGN, SSR, SPW, EPN, GYPP) (Table S4-5; Fig. 2c).

In the *xian* subgroup, haplotype analysis revealed that *OsAAP6* and *GW6* modulated vascular bundle-related traits without affecting quality or yield traits (Fig. 2c). Both *LP* and *DVB1* enhanced vascular bundle and increased SPW, but did not influence grain quality. *PAY1* influenced SVN and SVPA, while having no impact on PGWC, DEC, SPW and GYPP. *GS2* simultaneously influenced vascular bundle traits (LVPA and SVPA), grain quality-related traits (PGWC and DEC), and yield-related traits (TGN and SPW); however, the observed reduction in EPN offset potential gain in grain yield per plant. *GNP1* enhanced LVPA, SVPA, and TGW without affecting grain quality or yield. Conversely, *TGW6* and *DEP1* increased LVPA while decreasing PGWC and DEC, but did not influence yield traits (Fig. 2c). Overall, these results indicated that in the *xian* subgroup, a clear direct relationship between vascular bundle traits and yield or quality could not be established.

In *geng* subgroup, *LVPA4*, *FLO2*, *STRONG2*, *GL3.1*, *GW5*, *GW6*, *TGW6*, *DVB1*, and *MED14_1* collectively and positively regulated LVN, LVPA, PBN, TGN, and SPW, while simultaneously reducing EPN. Consequently, *LVPA4*, *FLO2*, *STRONG2*, *GL3.1*, and *GW5* exhibited no significant change in grain yield per plant, whereas *GW6*, *TGW6*, *DVB1*, and *MED14_1* resulted in decreased grain yield (Fig. 2c). Among them, *LVPA4*, *FLO2*, *GL3.1*, and *GW5* improved grain appearance quality by reducing PGWC and DEC, while *STRONG2*, *GW6*, *TGW6*, *DVB1* and *MED14_1* maintained stable grain quality (Fig. 2c). *RST1* enhanced LVN, LVPA, PBN, TGN, and SPW, and significantly increased grain yield per plant due to its negligible effect on EPN; meanwhile, it improved grain appearance rice quality (Fig. 2c). *PAY1* increased LVN but reduced SVPA, leading to higher PBN and TGN yet decreased grain quality, with no effect on SPW, EPN, and GYPP (Fig. 2c). Collectively, these findings indicate that, except for *PAY1*, the identified genes synergistically and positively regulate vascular bundle-related traits and SPW, contributing to improved appearance quality. However, due to the negative correlation between vascular bundle traits and EPN, enhancement

of peduncle vascular bundles alone may not directly increase grain yield per plant.

3.4. Genetic validation of RST1,LVPA4, GW5 and GL3.1 haplotypes

In the *geng* subgroup, *RST1* displayed a single nucleotide polymorphism (SNP) at position 28,588,881 bp on chromosome 6, distinguishing Hap2 from Hap3 (Fig. 3a). Hap3 was associated with significantly higher LVN (+19.52%), LVPA (+8.76%), PBN (+27.81%), TGN (+27.26%), GYPP (+14.00%), and SPW (+29.16%), while exhibiting lower PGWC (–42.36%) and DEC (–55.12%) compared with Hap2, identifying Hap3 as a superior haplotype positively associated with vascular bundle, yield, and grain quality (Fig. 3a; Table S6). A KASP marker, RST1_8881, was developed to distinguish the favorable (Hap3) and unfavorable allele (Hap2) of *RST1* (Table S7; Fig. S4). No significant difference was observed between Hap2 and Hap3 for SVN, SVPA, SBN, SSR, and EPN.

We constructed NIL-*RST1*^{PLUS} by introgressing the superior allele (Hap3) into the SI97 background, which carries the unfavorable allele Hap2 using marker-assisted selection with RST1_8881 (Fig. S5; Fig. 3b). Phenotypic analysis demonstrated that NIL-*RST1*^{PLUS} markedly enhanced LVN (+20.08%), LVPA (+20.00%), PBN (+19.85%), TGN (+10.62%), TGW (+7.54%), SPW (+16.96%), and GYPP (+17.54%), whereas SVN, SVPA, SBN, SSR, and EPN remained unaffected. Notably, NIL-*RST1*^{PLUS} reduced PGWC and DEC, improving grain appearance quality (Fig. 3c). Similarly, compared with Lemont, the *RST1* overexpression transgenic lines exhibited improvements in the above-mentioned vascular bundle and yield-related traits (Fig. S6). These findings corroborate the haplotype analysis, confirming its reliability.

LVPA4 exhibited a single nucleotide difference between Hap2 and Hap3 at position 31,212,801 bp on chromosome 4 in *geng* subgroup (Fig. 3d). Accessions carrying Hap3 exhibited significantly higher LVN (+17.38%), SVN (+13.40%), LVPA (+9.19%), SVPA (+34.13%), PBN (+21.59%), SBN (+42.89%), TGN (+29.96%) and SPW (+14.40%) but lower EPN (–13.04%), PGWC (–49.05%) and DEC (–51.47%) compared with Hap2, identifying Hap3 as an elite haplotype enhancing vascular bundle traits, SPW, and grain quality (Fig. 3d; Table S8). No significant differences were observed in TGW, SSR and GYPP. A KASP marker (LVPA4_2801) was developed to distinguish the favorable and unfavorable alleles of *LVPA4* (Table S7; Fig. S4). To validate these result*s*, two homozygous complementary transgenic lines were developed in the NK58 background (Fig. 3e). Compared with NK58, the two lines of *LVPA4* markedly enhanced LVN (+25.00%), SVN (+15.98%), LVPA (+10.54%), SVPA (+36.98%), PBN (+18.27%), SBN (+28.07%), TGN (+18.15%) and SPW (+36.86%), while TGW, SSR and GYPP remained unchanged. Notably, *LVPA4* also significantly reduced PGWC (–20.56%) and DEC (–36.76%), leading to an improved grain appearance quality (Fig. 3f). In our previous study, the NIL-*LVPA4* in Teqing background exhibited significantly increased vascular bundle area, secondary branch number, grain number per panicle, and ultimately grain yield compared with the recurrent parent Teqing [7].

Similarly, the superior alleles of *GW5* and *GL3.1* were also validated using NILs,

confirming their positive effects on target traits (Fig. S7). These results were consistent with the haplotype analysis, supporting their accuracy and reliability.

3.5. Construction of pyramiding-effect network of core genes

Among the candidate genes in *geng* subgroup, *LVPA4*, *GW5*, *FLO2* and *GL3.1* positively regulated vascular bundles, appearance grain quality, and single panicle weight without reducing grain yield per plant, whereas *RST1* enhanced vascular bundles, appearance grain quality, SPW, GYPP (Fig. 2c). Therefore, these five genes were selected as key candidates for simultaneous improvement of yield and appearance quality. All five genes were mainly expressed in both the stems and young panicles (Fig. S8). The spatial and temporal expression patterns of *FLO2* [25], *GW5* [18], *RST1* [35], *GL3.1* [17], and *LVPA4* [56] have been previously validated by RT-qPCR in published studies. The *GL3.1*, *LVPA4*, *FLO2*, *GW5*, and *RST1* were located on chromosomes 3, 4, 4, 5, and 6, respectively (Fig. S9a). Although *FLO2* and *LVPA4* are located on the same chromosome 4, no physical linkage was detected (Fig. S9b). Functional network analysis indicated that only LVPA4 and RST1 clustered together, with no direct genetic interaction (Fig. S9c). Yeast two-hybrid assays further showed that RST1-LVPA4, GL3.1-FLO2 and GL3.1-GW5 did not exhibit interactions (Fig. S10), and these results support the clustering trends observed in the functional network.

To assess their combined breeding potential, the pyramiding effects of the five genes (*LVPA4, RST1, GL3.1, FLO2* and *GW5*) were analyzed among 81 *geng* accessions from the 3K-RG dataset, which were classified into six groups based on the number of favorable alleles (Table S9). Interestingly, stacking more favorable alleles did not always result higher yield or better quality (Table S10; Fig. 4a), implying possible antagonistic or functional redundancy interactions among these genes. For instance, accessions carrying both *GW5* and *RST1* showed significantly higher GYPP compared with those carrying only one of the genes (+11.20% and +11.53%, respectively), indicating a synergistic effect. In contrast, *GL3.1* and *FLO2* displayed a negative pyramiding effect on GYPP (− 7.14%) (Fig. 4b; Table S11).

Based on these results, a gene pyramiding was constructed (Fig. 4c). *LVPA4* exhibited additive positive effects on quality traits, and synergistic effects with *GW5* and *RST1* on GYPP. *GW5* had additive positive effects with *LVPA4* and *RST1* on both GYPP and quality-related traits (PGWC and DEC), while it showed additive positive effects with *GL3.1* only on GYPP. *RST1* exhibited additive positive effects with *LVPA4*, *GW5*, *GL3.1*, and *FLO2* on grain quality related traits, but only with *LVPA4* and *GW5* on yield. *GL3.1* enhanced quality when combined with *LVPA4* or *RST1* and yield when combined with *GW5. FLO2* showed additive positive effects with *LVPA4* and *RST1* on grain quality. Collectively, these findings provide a theoretical framework for strategically introducing superior alleles to enhance both yield and quality.

3.6. Breeding potential of modern cultivars

A total of 221 officially released rice varieties from 1963 to 2023, ranging from 5

in the 1960s to 75 in the 2000s (Table S12; Fig. 5a). These varieties exhibited broad geographic representation, including five nationally certified varieties, 12 introduced from Japan, 15 recorded in the Chinese rice varieties and their pedigree [57], 15 registered in the Chinese National Crop Variety Register, and 174 from ten provinces or regions which range from 1 by Shanxi, Hebei and Yunnan to 134 by Heilongjiang (Fig. 5a). Twenty of these were identified as super rice varieties according to the Super Rice Varieties Directory 2025 (https://www.natesc.org.cn/) (Fig. 5a).

In addition to RST1_8881 for *RST1* and LVPA4_2801 for *LVPA4*, KASP markers GW5_5862, FLO2_1788, and GL3.1_6243 were developed to discriminate superior and inferior alleles of *GW5*, *FLO2*, and *GL3.1*, respectively, (Table S7; Fig. S4) based on haplotype-specific SNPs (Table S13–15). Among the 221 varieties, 205 (92.76%), 41 (18.55%), 12 (5.43%), and 19 (8.60%) carried the favorable alleles of *LVPA4*, *GW5*, *RST1*, and *FLO2*, respectively, whereas none carried the superior *GL3.1* allele (Table S16; Fig. 5b). Of these, 139 cultivars carried only *LVPA4*, 49 varieties carried two superior alleles of *LVPA4* and one of the other three genes mentioned above (33 with *LVPA4+GW5*, 2 with *LVPA4+RST1* and 14 with *LVPA4+FLO2*), seven contained *LVPA4*, *GW5*, and *RST1*, one possessed all superior alleles of the above four genes (*LVPA4+GW5+RST1+FLO2*), while 14 varieties carried none of the superior alleles (Fig. 5b). In both commercial and non-commercial cultivars, the utilization of favorable haplotype combinations (except for *LVPA4* alone) is generally low. However, commercial cultivars show increased frequencies of *LVPA4/GW5* (rising from 13.53% to 19.61%) and *LVPA4/RST1* (rising from 0.59% to 1.96%), while the proportion of genotypes lacking favorable alleles drops from 8.24% to 0.00% (Fig. 5c). Interestingly, only 6 super rice varieties and 23 commercial varieties carried two or more favorable alleles (Fig. 5d), indicating considerable potential for further genetic improvement.

Based on the gene pyramiding effect network and superior haplotype data, a molecular design breeding strategy was developed to enhance yield and quality in *geng* rice (Fig. 5e). For varieties carrying only *LVPA4*, the introduction of *GL3.1* could improve grain quality, while *RST1* and *GW5* would enhance both yield and quality. For *LVPA4* and *FLO2* backgrounds, adding *RST1* would enhance both traits. For *LVPA4* with *GW5* combinations, simultaneous incorporation of *GL3.1* and *RST1* would be most effective. In varieties with *LVPA4* and *RST1*, *GL3.1* would mainly increase quality, while *GW5* would enhance both yield and quality. Even in lines already pyramiding *LVPA4*, *GW5*, and *RST1*, incorporating *GL3.1* could further improve both yield and quality.

To experimentally validate this strategy, *RST1* was introduced into LG31 (carrying the favorable allele of *LVPA4*) to develop an introgression line (IL-*RST1*^{PLUS}) (Fig. 6a). The average sequencing depths of LG31 and IL-*RST1*^{PLUS} were 19.73× and 22.35×, respectively, with uniform coverage across all chromosomes (Fig. S11). A total of 140,514 common SNPs were detected between LG31 and IL-*RST1*^{PLUS} (Table S17), and sequence comparison indicated a background homozygosity of 93.06% (Fig. S12a). We detected three major donor-introgressed regions that were largely homozygous in the IL-*RST1*^{PLUS}, located on chromosome 8 (16.45–16.55 Mb) and chromosome 10 (21.20–21.30 Mb and 22.55–22.65 Mb) (Fig. S12b). There were no cloned genes

known to affect these traits within the three identified introgressed segments (Table S18), implying that the observed phenotypic differences between IL-*RST1*^{PLUS} and LG31 may primarily result from the introgression of *RST1* Compared with LG31, IL-*RST1*^{PLUS} exhibited significant increases in LVN, LVPA, and SVPA (Fig. 6b–e). Moreover, PBN, SBN, and TGN were markedly increased by 89.25%, 183.35%, and 101.64%, respectively (Fig. 6f–j). Although a reduction of 8.29% was observed in TGW (Fig. 6l), this was accompanied by increases in SPW and GYPP of 37.39% and 22.16%, respectively (Fig. 6m–n). Furthermore, *RST1* significantly reduced PGWC and DEC (Fig. 6o-q), resulting in a remarkable improvement in appearance quality.

We also constructed pyramiding lines NIL-(*GL3.1*+*GW5*)^{LT} that simultaneously carry the superior alleles of *GW5* and *GL3.1* from Lemont in Teqing background (carrying the unfavorable allele of the two genes) using marker-assisted selection. Compared with NIL-*GL3.1*^{LT} or NIL-*GW5*^{LT}, NIL-(*GL3.1*+*GW5*)^{LT} exhibited significantly increased PBN, SBN and GYPP, and significantly reduced PGWC and DEC (Fig. S7). In addition, the combined effect of *GW5* and *LVPA4* was confirmed in the collected developed *geng* cultivars (Fig. S13). These results validate the proposed breeding framework, demonstrating that the gene pyramiding network effectively enhances both yield and quality. Superior haplotype-carrying cultivars and three elite germplasms (91 UPLA, SP 6, and SKY BONNET) from the 3K panel were identified as potential donors for *geng* varieties improvement (Fig. S14).

4. Discussion

Rice production currently faces growing challenges in developing elite cultivars that combine high yield and superior grain quality to meet the demands of an expanding global population and rising living standards [1]. Establishing innovative breeding strategies to overcome the inherent trade-off between yield and quality is therefore essential for generating next-generation rice varieties with both attributes. Coordination of source, sink, and flow components is crucial in rice breeding. Agronomic improvement requires maintaining a strong source capacity (adequate assimilate and nutrient supply) and efficient transport capacity (unimpeded flow from source to sink), which together can partially overcome the trade-off between yield and grain quality, thereby enabling the simultaneous improvement of both traits [4]. Previous studies have frequently achieved gains in rice yield and grain quality by enhancing leaf-level photosynthetic capacity [6] or by modifying panicle-related traits [19,22,38,58]. However, relatively limited attention has been given to the improvement of vascular-bundle (flow), traits which could serve as a key strategy for breaking the yield–quality trade-off. Effective transport of photoassimilates from leaves and stems to grains by vascular bundle in the panicle peduncle is a necessary condition for improving grain filling and maximizing rice yield [59]. Mechanistically, vascular bundle traits may influence grain quality traits such as PGWC and DEC by regulating assimilate partitioning during grain filling, as vascular bundle structure determines the efficiency of assimilate transport and distribution from source to sink [5, 7, 9, 10]. In this study, we investigated the correlation between peduncle vascular bundles characteristics, yield

and grain quality, and further discussed the potential application of pyramiding related important genes to improve yield and quality in *geng* subgroup.

The rice 3K RG panel, with extensive natural variation and a wide array of superior alleles, serves as a valuable genetic resource for exploring haplotype diversity. The panel can be broadly classified into five subgroups *xian*, *geng*, *admix*, *aus* and *basmati,* among which *xian* and *geng* represent the predominant subgroups [26]. There are substantial differences in the vascular bundle system between *xian* and *geng* subgroups, and the vascular bundle system is an important parameter that defines differentiation between the two subspecies [60]. The panel of 248 accessions from 3K RG, including 167 *xian* accessions and 81 *geng* accessions, employed in this study, to ensure both the robustness of agronomic trait evaluation and the genetic diversity of the dataset (Table S1; Fig. 1a-b), thereby enhancing the robustness and generalizability of the analysis results. Although multi-year and multi-environment evaluations are generally important for complex traits such as yield and grain quality, the consistent trait distributions across two different ecological zones and the predominance of genotype effects indicate that the associations identified here are robust at the population level (Fig. S2). while further validation under broader environmental conditions will be valuable.

Xian varieties generally exhibit a larger LVN in the peduncle compared with *geng* varieties [60], whereas their LVPA is significantly smaller [61]. Consistent with previous findings, our results demonstrated that the peduncle LVN in *xian* varieties was 36.01% higher, and the LVPA was 7.95% lower, than in *geng* cultivars (Fig. 1c). Furthermore, previous studies have reported significant differences between *xian* and *geng* subgroup in PBN [62], TGW [63] and GYPP [64], which are consistent with the results of the present study (Fig. 1c). Many cloned genes, such as *GL3.1* [17], *GW5* [65], *LVPA4* [7], *TGW6* [32], *PAY1* [34], *Gn1a* [66], and *sd1* [67], also exhibit clear subpopulation differentiation in their haplotypes, which were consistent with our findings (Table S3; Fig. 2b). These results indicated that different agronomic traits exhibited significant genetic differences between *xian* and *geng* subgroups. Therefore, analyses of genetic associations and inter-trait relationships (e.g., between vascular bundles, yield and quality), should be conducted separately within each subgroup, rather than across a mixed population.

The phloem of peduncle vascular bundles is responsible for assimilate transport from leaves to grains and the number of vascular bundles is significantly positively correlated with PBN and TGN. Both the phloem area and the number of vascular bundles jointly determine nutrient transport efficiency and play a decisive role in yield and grain quality formation [7,8]. Larger LVPA can improve the efficiency of assimilate transport and carbohydrate supply to developing grains, thereby promoting uniform and sufficient grain filling, which ultimately reduces grain chalkiness. Some genes, such as *FZP, PAY1*, *GW5*, and *FLO2*, exhibit significant differences in large vascular bundle number among their distinct haplotypes, suggesting their potential involvement in regulating vascular bundle trait. However, no such function has been identified for these genes to date, and the underlying mechanisms by which they might regulate vascular traits remain unclear. Although a superior vascular bundle-related

trait was generally associated with improved grain quality (PGWC and DEC) and an increase in SPW in both *xian* and *geng* subgroups, this advantage was offset in the grain yield per plant due to significant negative correlation between vascular bundle traits and EPN. The negative correlations between vascular bundle traits and EPN in *geng* likely reflect a resource allocation trade-off between panicle number and panicle size. Grain yield components in rice are known to exhibit compensatory relationships, where increases in spikelet number or panicle size are often accompanied by reductions in panicle number due to source-sink balance and assimilate allocation constraints. Enhanced vascular bundle capacity may promote assimilate transport and grain filling, thereby increasing single panicle weight (SPW), but this advantage may be partially offset by reduced panicle number, leading to weaker effects on grain yield per plant [68].

Consequently, vascular bundle traits were negatively correlated with grain yield per plant in *geng* subgroup, whereas in *xian* group the correlation was relatively weak (Fig. 1d-e). This result was further confirmed by the haplotype results of 11 genes (*LVPA4, FLO2, STRONG2, GL3.1, GW5, GW6, TGW6, DVB1, MED14_1, RST1* and *PAY1*) related to vascular bundle traits in *geng* subgroup (Fig. 2c). In contrast, in *xian*, the haplotype results of nine genes (*OsAAP6, GW6, LP, PAY1, DVB1, GS2, GNP1, TGW6* and *DEP1*) associated with vascular bundle traits did not show an obvious correlation between vascular bundle traits and single panicle weight or quality-related traits (Fig. 2c). Validation through the development of near-isogenic lines (NILs) and complementary transgenic lines for *LVPA4* (Fig. 3d-e), *RST1* (Fig. 3a-c), *GW5* (Fig. S7) and *GL3.1* (Fig. S7) confirmed the reliability and accuracy of these haplotype results. In future, we will focus on the functional characterization of *FLO2*, which was not experimentally validated in this study. These findings underscore the crucial role of vascular bundle traits in breaking the yield–quality trade-off within *geng* rice, as they enhance SPW and grain quality without compromising either. Balancing vascular bundles traits with EPN is therefore vital for achieving simultaneous improvement in yield and quality. Importantly, the distinct patterns observed between *xian* and *geng* are consistent with previous reports showing subspecies-specific genetic architectures and trait relationships in rice [7,69,70].. *Geng* rice generally has smaller panicles but more tillers, whereas *xian* rice tends to have larger panicles with fewer tillers [71,72]. This architectural difference may make vascular bundle capacity a more direct determinant of grain filling and quality in *geng*, while in *xian* compensatory mechanisms associated with larger panicles may buffer vascular variation effects, leading to more complex trait relationships. Therefore, further investigation into the genetic basis and regulatory networks of vascular bundle development may provide valuable insights for designing breeding strategies that optimize both yield and quality across rice subspecies. However, due to the experimental cycle and the limitations of available materials, such investigations were beyond the scope of this study. While this study focuses on flow-sink related genetic regulation, source-related processes such as photosynthetic capacity and non-structural carbohydrate accumulation also contribute to yield formation, highlighting the importance of coordinated source-sink interactions in future studies.

Haplotype analysis identified five key genes with potential for breeding applications, including *GL3.1*, *GW5*, *RST1*, *FLO2* and *LVPA4* in *geng* group, which simultaneously enhanced vascular bundle traits, grain quality, and SPW, without compromising the grain yield per plant (Fig. 2c). *GL3.1* regulates the cell cycle to optimize grain shape and yield [17], whereas *LVPA4* increased the phloem area of vascular bundles in panicle peduncle, thereby improving assimilate transport efficiency and ultimately promoting both the number of filled grains per panicle and the thousand-grain weight [7], suggested that *LVPA4* is a key gene for yield and quality improvement with considerable breeding potential. Similarly, *RST1* contributed to enhance stress tolerance and resource use efficiency, indirectly influencing yield and quality [35]. Variations in *GW5* led to substantial changes in grain shape and yield, underscoring its importance for grain shape improvement and yield enhancement [18]. *FLO2*, by modulating panicle architecture and fertility, indirectly affected yield and thus represented a promising target for breeding improvement [25]. Collectively, these genes are essential regulators of yield, quality, and vascular bundle related traits in *geng* rice. Despite this, most findings remain at the theoretical stage, with limited practical integration into breeding programs. Analysis of the 221 released *geng* varieties revealed that the superior allele of *LVPA4* had already been extensively deployed in breeding programs, whereas the superior allele of *GW5* was only present in approximately 20% of the varieties. In contrast, the number of varieties carrying the superior alleles of *RST1* and *FLO2* remained quite limited, and the favorable allele of *GL3.1* was completely absent in the cultivars surveyed (Fig. 5b). These findings highlighted the unequal adoption of yield and quality-related alleles in *geng* breeding and suggested that substantial untapped genetic potential. The underutilization of certain key alleles provides opportunities for future breeding strategies to achieve synergistic improvements in both yield and grain quality, thereby further advancing the genetic enhancement of *geng* subgroup.

Although these five genes (*GL3.1*, *GW5*, *FLO2*, *LVPA4* and *RST1*) exhibited neither physical linkage (Fig. S9a-b) nor protein-protein interactions (Fig. S9c), their pyramiding was not always beneficial (Fig. 4a), as certain combinations exhibited negative pyramiding effects (Fig. 4b). Currently, there are no reports indicating functional interactions between these genes, and the underlying mechanism of this negative interaction remains unclear. Further studies are needed to elucidate the molecular basis of such unexpected effects. Detailed analysis of these pyramiding effects enabled the construction of a gene interaction network to facilitate concurrent improvement of yield and quality (Fig. 4c). A collection of superior alleles, functional markers, and pyramiding strategies for the molecular design breeding of *geng* rice has been developed. The complex population structure of the diverse germplasm panel may influence the estimation of gene effects; nevertheless, the identified superior allele combinations provide a useful foundation for molecular design breeding and warrant further validation in controlled genetic backgrounds. We can strategically introduce new favorable alleles into various rice varieties to further enhance yield and quality, based on the presence of superior alleles identified in 221 cultivated varieties (Fig. 5). The effectiveness of the proposed breeding strategy was supported by the pyramiding

of *RST1* with *LVPA4* and *GW5* with *GL3.1* through introgression lines and NILs. In the future, we will verify the synergistic effects of these pyramiding lines through experiments in different genetic backgrounds and multiple environments to confirm their breeding applicability in a broader ecological region. Due to the large allelic diversity in the population, only representative allele combinations were experimentally validated. These results support the reliability of the haplotype-based approach and suggest its potential utility for prioritizing favorable allele combinations in molecular breeding. Further validation of additional genes using NILs or transgenic approaches will be important for elucidating their mechanistic roles and will be pursued in future studies.

Together, our findings establish an integrative framework linking flow genetics with molecular breeding strategies, providing practical targets for next-generation high-yield, high-quality *geng* rice improvement. To better illustrate this framework, we propose a conceptual model integrating source-flow-sink relationships and the regulatory hierarchy linking vascular bundle architecture, assimilate transport, and grain quality (Fig. 7). However, because about 6.94% of the genome in IL-*RST1*^{PLUS} originated from the donor, it is possible that linked donor loci contributed to or modified the phenotype, even though no cloned genes known to affect these traits were detected within the identified introgressed segments. Thus, further verification through the development of additional introgression lines and multi-environment trials will be necessary before large-scale breeding applications. Such studies are needed to fully assess the environmental stability of these associations and potential genotype-by-environment interactions. As this represents a long-term endeavor, future research will focus on validating these key genes in diverse *geng* backgrounds, integrating them into modern breeding pipelines, and addressing challenges related to stability, pleiotropy, and background dependency to fully realize their potential in high-yield, high-quality rice improvement. This study establishes a comprehensive genetic framework connecting vascular bundle architecture with yield-quality coordination and delivers practical molecular tools for next-generation improvement of *geng* rice. Integrating vascular-bundle genomics with digital phenotyping and predictive breeding offers a forward-looking strategy to design rice ideotypes optimized for both yield and grain quality, and provides a conceptual basis for parallel advancements in other crops such as wheat and maize.

5. Conclusion

This study establishes a comprehensive genetic framework linking vascular bundle architecture with the coordination of yield and grain quality in *geng* rice. Through integrated haplotype analysis, functional validation, and gene pyramiding, five key genes (*GL3.1*, *GW5*, *FLO2*, *LVPA4*, and *RST*1) were identified as synergistic regulators that enhance vascular bundle development, single-panicle weight, and grain appearance quality without compromising yield. Pyramiding analysis and introgression-line validation confirmed that specific allele combinations produce additive or synergistic effects, providing an empirical basis for flow-centered molecular design breeding. These findings highlight the potential of optimizing vascular transport

capacity ("flow trait") as a new dimension for breaking the traditional yield-quality trade-off. The developed functional markers and pyramiding strategies provide a practical molecular tool and a conceptual framework for the next generation of high-yield, high-quality *geng* rice breeding, providing a reference for similar improvements in other cereal crops such as wheat and maize.

Trait abbreviations

LVN, number of large vascular bundles; SVN, number of small vascular bundles; LVPA, phloem area of large vascular bundles; SVPA, phloem area of small vascular bundles; EPN, effective panicle number per plant; PBN, primary branch number; SBN, secondary branch number; TGN, total grain number per panicle; SSR, seed setting rate; TGW, thousand grain weight; GYPP, grain yield per plant; SPW, single panicle weight; PGWC, percentage of grains with chalkiness; DEC, degree of chalkiness.

References

[1] Ishfaq J, Soomar AM, Khalid F, et al. Assessing rice (*oryza sativa* L.) quality: a comprehensive review of current techniques and future directions. J Agric Food Res 2023;14. https://doi.org/10.1016/j.jafr.2023.100843.

[2] Takatsuji H. Regulating Tradeoffs to Improve Rice Production. Front Plant Sci 2017;28:171. https://doi.org/10.3389/fpls.2017.00171..

[3] Cao S, Liu B, Wang D, et al. Orchestrating seed storage protein and starch accumulation toward overcoming yield-quality trade-off in cereal crops. J Integr Plant Biol 2024;66(3):468–483. https://doi.org/10.1111/jipb.13633

[4] Ueda T, Taniguchi Y, Adachi S, et al. Gene Pyramiding Strategies for Sink Size and Source Capacity for High-Yield *Japonica* Rice Breeding. Rice 2025;18(1):6. https://doi.org/10.1186/s12284-025-00756-w.

[5] Cui KH, Peng SB, Xing YZ, et al. Molecular dissection of the genetic relationships of source, sink and transport tissue with yield traits in rice. Theor Appl Genet 2003;106(4):649–658. https://doi.org/10.1007/s00122-002-1113-z.

[6] Croce R, Carmo-Silva E, Cho YB, et al. Perspectives on improving photosynthesis to increase crop yield. Plant Cell 2024;36(10):3944–3973. https://doi.org/10.1093/plcell/koae132.

[7] Zhai L, Yan A, Shao K, et al. *Large Vascular Bundle Phloem Area 4* enhances grain yield and quality in rice via source-sink-flow. Plant Physiol 2023;191(1):317–334. https://doi.org/10.1093/plphys/kiac461.

[8] You C, Wang H, Huang Y, et al. Relationship Between the Vascular Bundle Structure of Panicle Branches and the Filling of Inferior Spikelets in Large-Panicle Japonica Rice. Front. Plant Sci 2021;12:774565. https://doi.org/10.3389/fpls.2021.774565.

[9] Li G, Hu Q, Zhang G, et al. Sucrose Unloading in Grains Modulates the Disparity in Grain Filling of Superior and Inferior Spikelets in Rice. Physiol Plant. 2026;178(1):e70809. https://doi.org/10.1111/ppl.70809.

[10] Li G, Chen X, Zhou C, et al. Vascular Bundle Characteristics of Different Rice Variety Treated with Nitrogen Fertilizers and Its Relation to Stem Assimilates Allocation and Grain Yield. Agriculture 2022;12(6), 779. https://doi.org/10.3390/agriculture12060779.

[11] Zhang Y, Han E, Peng Y, et al. Rice co-expression network analysis identifies gene modules associated with agronomic traits. Plant Physiol 2022;190(2):1526–1542. https://doi.org/10.1093/plphys/kiac339.

[12] Huangfu L, Chen R, Lu Y, et al. *OsCOMT*, encoding a caffeic acid O-methyltransferase in melatonin biosynthesis, increases rice grain yield through dual regulation of leaf senescence and vascular development. Plant Biotechnol J 2022;20(6):1122–1139. https://doi.org/10.1111/pbi.13794.

[13] Malik N, Ranjan R, Parida SK, et al. Mediator subunit OsMED14_1 plays an important role in rice development. Plant J 2020;101(6):1411–1429. https://doi.org/10.1111/tpj.14605.

[14] Zhang L, Feng P, Deng Y, et al. *Decreased Vascular Bundle 1* affects mitochondrial and plant development in rice. Rice 2021;14(1):13. https://doi.org/10.1186/s12284-021-00454-3.

[15] Li M, Tang D, Wang K, et al. Mutations in the F-box gene *LARGER PANICLE* improve the panicle architecture and enhance the grain yield in rice. Plant Biotechnol J 2011;9(9):1002–1013. https://doi.org/10.1111/j.1467-7652.2011.00610.x.

[16] Zhao Y, Wang X, Gao J, et al. The MYB61-STRONG2 module regulates culm diameter and lodging resistance in rice. J Integr Plant Biol 2025;67(2):243–257. https://doi.org/10.1111/jipb.13830.

[17] Qi P, Lin YS, Song XJ, et al. The novel quantitative trait locus *GL3.1* controls rice grain size and yield by regulating Cyclin-T1;3. Cell Res 2012;22(12):1666–1680. https://doi.org/10.1038/cr.2012.151.

[18] Liu J, Chen J, Zheng X, et al. *GW5* acts in the brassinosteroid signalling pathway to regulate grain width and weight in rice. Nat Plants 2017;3:17043. https://doi.org/10.1038/nplants.2017.43..

[19] Ashikari M, Sakakibara H, Lin S, et al. Cytokinin oxidase regulates rice grain production. Science 2005;309(5735):741–745. https://doi.org/10.1126/science.1113373.

[20] Su S, Hong J, Chen X, et al. Gibberellins orchestrate panicle architecture mediated by DELLA-KNOX signalling in rice. Plant Biotechnol J 2021;19(11):2304–2318. https://doi.org/10.1111/pbi.13661.

[21] Miura K, Ikeda M, Matsubara A, et al. *OsSPL14* promotes panicle branching and higher grain productivity in rice. Nat Genet 2010;42(6):545–549. https://doi.org/10.1038/ng.592.

[22] Huang H, Ye Y, Song W, et al. Modulating the C-terminus of DEP1 synergistically enhances grain quality and yield in rice. J Genet Genomics 2022;49(5):506–509. https://doi.org/10.1016/j.jgg.2022.01.009.

[23] Wu B, Yun P, Zhou H, et al. Natural variation in *WHITE-CORE RATE 1* regulates redox homeostasis in rice endosperm to affect grain quality. Plant Cell 2022;234(5):1912–1932. https://doi.org/10.1093/plcell/koac057.

[24] Li Y, Fan C, Xing Y, et al. *Chalk5* encodes a vacuolar H^+-translocating pyrophosphatase influencing grain chalkiness in rice. Nat Genet 2014;46(4):398–404. https://doi.org/10.1038/ng.2923.

[25] She KC, Kusano H, Koizumi K, et al. A novel factor *FLOURY ENDOSPERM2* is involved in regulation of rice grain size and starch quality. Plant Cell 2010;22(10):3280–3294. https://doi.org/10.1105/tpc.109.070821.

[26] Wang W, Mauleon R, Hu Z, et al. Genomic variation in 3,010 diverse accessions of Asian cultivated rice. Nature 2018;557(7703):43–49. https://doi.org/10.1038/s41586-018-0063-9.

[27] Qian Q. Rice Breeding: A Long Noncoding Locus with Great Potential. Molecular Plant 2019;12(11):1431–1433. https://doi.org/10.1016/j.molp.2019.10.008.

[28] Wang W, Wang W, Pan Y, et al. A new gain-of-function *OsGS2/GRF4* allele generated by CRISPR/Cas9 genome editing increases rice grain size and yield. Crop J 2022;10(4):1207–1212. https://doi.org/10.1016/j.cj.2022.01.004.

[29] Li Y, Fan C, Xing Y, et al. Natural variation in *GS5* plays an important role in regulating grain size and yield in rice. Nat Genet 2011;43(12):1266–1269. https://doi.org/10.1038/ng.977.

[30] Shi CL, Dong NQ, Guo T, et al. A quantitative trait locus *GW6* controls rice grain size and yield through the gibberellin pathway. Plant J 2020;103(3):1174–1188. https://doi.org/10.1111/tpj.14793.

[31] Song XJ, Kuroha T, Ayano M, et al. Rare allele of a previously unidentified histone H4 acetyltransferase enhances grain weight, yield, and plant biomass in rice. Proc Natl Acad Sci U S A 2015;112(1):76–81. https://doi.org/10.1073/pnas.1421127112.

[32] Ishimaru K, Hirotsu N, Madoka Y, et al. Loss of function of the IAA-glucose hydrolase gene *TGW6* enhances rice grain weight and increases yield. Nat Genet 2013;45(6):707–711. https://doi.org/10.1038/ng.2612.

[33] Chen Q, Tian F, Cheng T, et al. Translational repression of *FZP* mediated by CU-rich element/OsPTB interactions modulates panicle development in rice. Plant J 2022;110(5):1319–1331. https://doi.org/10.1111/tpj.15737.

[34] Zhao L, Tan L, Zhu Z, et al. *PAY1* improves plant architecture and enhances grain yield in rice. Plant J 2015;83(3):528–536. https://doi.org/10.1111/tpj.12905.

[35] Deng P, Jing W, Cao C, et al. Transcriptional repressor RST1 controls salt tolerance and grain yield in rice by regulating gene expression of asparagine synthetase. Proc Natl Acad Sci U S A 2022;119(50):e2210338119. https://doi.org/10.1073/pnas.2210338119.

[36] Wu Y, Wang Y, Mi XF, et al. The QTL *GNP1* Encodes GA20ox1, Which Increases Grain Number and Yield by Increasing Cytokinin Activity in Rice Panicle Meristems. PLoS Genet 2016;12(10):e1006386. https://doi.org/10.1371/journal.pgen.1006386.

[37] Ruan B, Shang L, Zhang B, et al. Natural variation in the promoter of *TGW2* determines grain width and weight in rice. New Phytol 2020;227(2):629–640. https://doi.org/10.1111/nph.16540.

[38] Wang H, Zhang Y, Sun L, et al. *WB1*, a Regulator of Endosperm Development in Rice, Is Identified by a Modified MutMap Method. Int J Mol Sci 2018;19(8):2159. https://doi.org/10.3390/ijms19082159.

[39] Wang S, Wu K, Yuan Q, et al. Control of grain size, shape and quality by *OsSPL16* in rice. Nat Genet 2012;44(8):950–954. https://doi.org/10.1038/ng.2327..

[40] He L, Chen T, Liang W, et al. The RING-Type Domain-Containing Protein GNL44 Is Essential for Grain Size and Quality in Rice (*Oryza sativa* L.). Int J Mol Sci 2024;25(1):589. https://doi.org/10.3390/ijms25010589.

[41] Masayuki I, Yasuyuki M, Aya T, et al. *Du3*, a mRNA cap-binding protein gene, regulates amylose content in *japonica* rice seeds. Plant Tissue Cult Lett 2008;25(5):483–487. https://doi.org/10.1016/j.fm.2004.01.015.

[42] Peng B, Kong H, Li Y, et al. *OsAAP6* functions as an important regulator of grain protein content and nutritional quality in rice. Nat Commun 2014;5:4847. https://doi.org/10.1038/ncomms5847.

[43] Alexandrov N, Tai S, Wang W, et al. SNP-Seek database of SNPs derived from 3000 rice genomes. Nucleic Acids Res 2015;43:D1023–D1027. https://doi.org/10.1093/nar/gku1039

[44] Purcell S, Neale B, Todd-Brown K, et al. PLINK: a tool set for whole-genome association and population-based linkage analyses. Am J Hum Genet 2017;81(3):559–75. https://doi.org/10.1086/519795

[45] Wang Y, Wang XQ, Zhai L, Chen K, et al. A novel *Effective Panicle Number per Plant 4* haplotype enhances grain yield by coordinating panicle number and grain number in rice. The Crop Journal 2023;12(1):202–212. https://doi.org/10.1016/j.cj.2023.11.003.

[46] Dong SS, He WM, Ji JJ, et al. LDBlockShow: a fast and convenient tool for visualizing linkage disequilibrium and haplotype blocks based on variant call format files. Brief Bioinform 2021;22(4):bbaa227. https://doi.org/10.1093/bib/bbaa227.

[47] Dipta B, Sood S, Mangal V, et al. KASP: a high-throughput genotyping system and its applications in major crop plants for biotic and abiotic stress tolerance. Mol Biol Rep 2024;51(1):508. https://doi.org/10.1007/s11033-024-09455-z.

[48] Murray MG, Thompson WF. Rapid isolation of high molecular weight plant DNA. Nucleic Acids Res 1980;8(19):4321–4325. https://doi.org/10.1093/nar/8.19.4321

[49] Metzker, ML. Sequencing technologies-the next generation (with notes). Nat Rev Genet 2009;11(1):31–46. https://doi.org/10.1038/nrg2626.

[50] McKenna A, Hanna M, Banks E, et al. The Genome Analysis Toolkit: a MapReduce framework for analyzing next-generation DNA sequencing data. Genome Res 2010;20(9):1297–1303. https://doi.org/10.1101/gr.107524.110.

[51] McNally KL, Childs KL, Bohnert R, et al. Genomewide SNP variation reveals relationships among landraces and modern varieties of rice. Proc Natl Acad Sci U S A 2009;106(30):12273–12278. https://doi.org/10.1073/pnas.0900992106.

[52] Zeng D, Tian Z, Rao Y, et al. Rational design of high-yield and superior-quality rice. Nat Plants 2017;3:17031. https://doi.org/10.1038/nplants.2017.31

[53] Waqas MAB, Awan MJA, Amin I, et al. Engineering high yield basmati rice by editing multiple negative regulators of yield. Mol Biol Rep 2025;52(1):545. https://doi.org/10.1007/s11033-025-10660-7

[54] Abbai R, Singh VK, Nachimuthu VV, et al. Haplotype analysis of key genes governing grain yield and quality traits across 3K RG panel reveals scope for the development of tailor-made rice with enhanced genetic gains. Plant Biotechnol J 2019;17(8):1612–1622. https://doi.org/10.1111/pbi.13087

[55] Kumar S, Stecher G, Li M, et al. MEGA X: Molecular Evolutionary Genetics Analysis across Computing Platforms. Mol Biol Evol 2018;35(6):1547–1549. https://doi.org/10.1093/molbev/msy096.

[56] Qi J, Qian Q, Bu Q, et al. Mutation of the rice Narrow leaf1 gene, which encodes a novel protein, affects vein patterning and polar auxin transport. Plant Physiol 2008;147(4):1947-1959. https://doi:10.1104/pp.108.118778

[57] Lin SC. Rice varieties in China and their pedigrees. Shanghai Scientific and Technical Publishers 1991.

[58] Guo T, Si F, Lu F, et al. Competitive binding of small antagonistic peptides to the OsER1 receptor optimizes rice panicle architecture. Plant Commun 2025;6(3):101204. https://doi.org/10.1016/j.xplc.2024.101204

[59] Mathan J, Singh A, Ranjan A. Sucrose transport and metabolism control carbon partitioning between stem and grain in rice. J Exp Bot 2021;72(12):4355–4372. https://doi.org/10.1093/jxb/erab066.

[60] Fei C, Geng X, Xu Z, et al. Multiple areas investigation reveals the genes related to vascular bundles in rice. Rice 2019;12(1):17. https://doi.org/10.1186/s12284-019-0278-x.

[61] Zhai L, Zheng T, Wang X, et al. QTL mapping and candidate gene analysis of peduncle vascular bundle related traits in rice by genome-wide association study. Rice 2018;11(1):13. https://doi.org/10.1186/s12284-018-0204-7.

[62] Bai X, Zhao H, Huang Y, et al. Genome-Wide Association Analysis Reveals Different Genetic Control in Panicle Architecture Between and Rice. Plant Genome 2016;9(2). https://doi.org/10.3835/plantgenome2015.11.0115.

[63] Li R, Li M, Ashraf U, et al. Exploring the Relationships Between Yield and Yield-Related Traits for Rice Varieties Released in China From 1978 to 2017. Front Plant Sci 2019;10:543. https://doi.org/10.3389/fpls.2019.00543.

[64] Liu Y, Zhang S, Qian H, et al. Variation in a single allele drives divergent yield responses to elevated CO2 between rice subspecies. Nat Commun 2025;216(1):376. https://doi.org/10.1038/s41467-024-55809-3.

[65] Weng J, Gu S, Wan X, et al. Isolation and initial characterization of *GW5*, a major QTL associated with rice grain width and weight. Cell Res 2008;18(12):1199–1209. https://doi.org/10.1038/cr.2008.307.

[66] Wang J, Xu H, Li N, et al. Artificial Selection of *Gn1a* Plays an Important role in Improving Rice Yields Across Different Ecological Regions. Rice 2015;8(1):37. https://doi.org/10.1186/s12284-015-0071-4.

[67] Rana BB, Kamimukai M, Bhattarai M, et al. Effects of tall alleles *SD1-in* and *SD1-ja* to the dwarfing allele sd1-d originating from 'Dee-geo-woo-gen' on yield and related traits on the genetic background of *indica* IR36 in rice. Breed Sci 2021;71(3):334–343. https://doi.org/10.1270/jsbbs.21001.

[68] Paul MJ, Watson A, Griffiths CA. Linking fundamental science to crop improvement through understanding source and sink traits and their integration for yield enhancement. J Exp Bot 2020;71(7):2270–2280. https://doi.org/10.1093/jxb/erz480

[69] Liao S, Yan J, Xing H, et al. Genetic basis of vascular bundle variations in rice revealed by genome-wide association study. Plant Sci 2021;302:110715. https://doi.org/10.1016/j.plantsci.2020.110715.

[70] Li G, Chen X, Zhou C, et al. Vascular Bundle Characteristics of Different Rice Variety Treated with Nitrogen Fertilizers and Its Relation to Stem Assimilates Allocation and Grain Yield. Agriculture 2022;12(6):779. https://doi.org/10.3390/agriculture12060779.

[71] Fukushima A. Varietal differences in tiller and panicle development determining the total number of spikelets per unit area in rice. Taylor & Francis 2019(2). https://doi.org/10.1080/1343943X.2018.1562308.

[72] Takai T. Potential of rice tillering for sustainable food production. J Exp Bot 2024;75(3):708–720. https://doi.org/10.1093/jxb/erad422

Figure captions

Fig. 1. Phenotypic variation of 248 accessions and correlations among fourteen agronomic traits. (a) Origins of accessions. (b) Phylogenetic tree by NJ method. (c) Phenotypic distribution of fourteen traits in *xian* (n=167) and *geng* (n=81) subgroups. *, ** and *** denote the significance of Student's *t*-test at $p < 0.05$, 0.01 and 0.001 between *xian* and *geng*, respectively. n.s. denote insignificance at the 0.05 level. Correlations among fourteen evaluated traits in *xian* (n=167) (d) and *geng* (n=81) (e) group. The values are correlation coefficients. The areas and colors of ellipses correspond to absolute values of the corresponding *r*. Right and left oblique ellipses indicate positive and negative correlations, respectively. Values without glyphs are insignificant at the 0.05 probability level. *, **, and *** represent significant correlations at $p < 0.05$, 0.01, and 0.001, respectively. Abbreviations of traits are listed at the end of the article and are used throughout all figures .

Fig. 2. Haplotypes of 31 cloned genes. (a) The 31 genes used in this study. (b) Haplotype analysis of 31 genes in four vascular bundle related traits in the whole, *xian*, and *geng* groups. Numbers indicate major haplotypes per gene, and sector size reflects haplotype number. Panels represent different traits, and colors indicate significance levels among haplotypes (see legend). "NA" indicates only one haplotype was detected and ANOVA was not performed.. (c) Haplotype of genes affecting vascular bundle related traits in *xian* and *geng* group for yield- and quality-related traits. Blue with "+" indicates a significant increase, green with "-" indicates a significant decrease, and yellow with "0" indicates no significant difference.

Fig. 3. Genetic verification of the haplotype of *RST1* and *LVPA4*. (a) Haplotype of *RST1* in *geng* group. (b) Plant performance of SI97 and near-isogenic line NIL-*RST1*^{PLUS}. (c) Phenotypic performance of fourteen traits in SI97 and NIL-*RST1*^{PLUS}. (d) Haplotype of *LVPA4* in *geng* group. (e) Plant performance of NK58 and complementary transgenic materials (NK58+*LVPA4*^{LT}). (f) Phenotypic performance of fourteen traits in NK58 and NK58+*LVPA4*^{LT}. Data are presented as mean ± SD (n = 3). *, ** and *** denote the significance of Student's *t*-test at $p < 0.05$, 0.01 and 0.001. n.s. denote insignificance at the 0.05 level.

Fig. 4. The pyramid effect analysis among the superior alleles. (a) The pyramid effect with different number of superior alleles. The x-axis indicates the number of pyramided favorable alleles (0-5), and numbers on the plot represent phenotypic values. Sample sizes for each category (0-5 favorable alleles) were 12, 34, 14, 12, 4, and 5, respectively. Different letters indicate significant differences at the 0.05 level. Dashed lines indicate trend lines. (b) Analysis of pairwise pyramiding effects among *RST1*, *LVPA4*, *GL3.1*, *GW5* and *FLO2*. "+" and "－" on thr x-axis indicate the presence and absence of the superior allele of the genes, respectively. Dashed lines indicate trend lines. Detailed *p* values and sample sizes (n) for each allele combination are provided in Table S11. (c) The relationships among *LVPA4*, *RST1*, *GL3.1*, *FLO2* and *GW5*. Line colors represent the pyramiding effects between gene pairs. Solid lines and dashed lines represent appearance quality and grain yield per plant, respectively. Haplotype labels on each gene denote the superior haplotypes.

Fig. 5. Identification and breeding application of superior alleles in 221 modern released *geng* varieties. (a) Information of collected 221 modern released varieties. (b) The distribution of commercial varieties in the released varieties. (c) Frequency distribution of gene combinations in commercial and non-commercial varieties. (d) Identification of the superior alleles carried by the super rice varieties and commercial varieties. (e) The five genes' applications in breeding of 221 modern released varieties.

Fig. 6. Genetic verification of the breeding application of *RST1* through evaluation of an introgression line. (a) Development of introgression line IL-*RST1*^{PLUS}. Phenotypic identification of peduncle vascular bundle (b-e), yield (f-n), and appearance quality (o-q) related traits. Data are presented as mean ± SD (n = 3). *, ** and *** denote the significance of Student's *t*-test at $p < 0.05$, 0.01 and 0.001 between SI97 and IL-*RST1*^{PLUS}. n.s. denote insignificance at the 0.05 level.

Fig. 7. Conceptual model of source-flow-sink coordination underlying the effects of peduncle vascular bundle architecture on grain yield and quality.

Highlights

1. Vascular bundle architecture was identified as a key regulator enabling concurrent improvement of grain yield and appearance quality in *geng* rice.
2. Five key genes (*GL3.1*, *GW5*, *FLO2*, *LVPA4*, and *RST1*) were identified as synergistic regulators enhancing vascular development, panicle weight, and grain quality without compromising yield.
3. A pyramiding-effect gene network was constructed, and superior haplotypes were developed into KASP markers for breeding applications.
4. The uneven distribution of superior alleles among modern cultivars highlights the need for targeted breeding strategies.
5. The flow-centered molecular design strategy for yield-quality coordination was validated by introgression lines.

Graphical Abstract

Click here to access/download;Graphical Abstract;Graphical Abstract_01.png

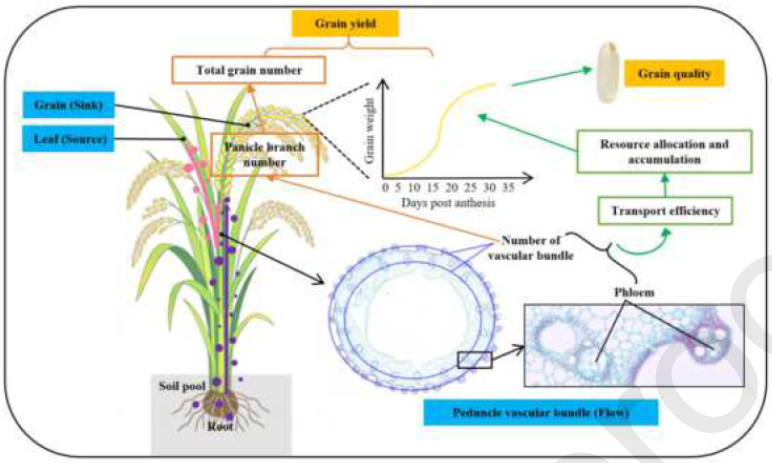

Compliance with ethics requirement

All the authors state that this article does not contain any studies with human or animal subjects.

Declaration of competing interest

The authors declare that they have no known competing financial interests or personal relationships that could have appeared to influence the work reported in this paper.

Figure (300dpi and editable format)

Click here to view linked References

Click here to access/download:Figure (300dpi and editable format);Fig. 1.pdf

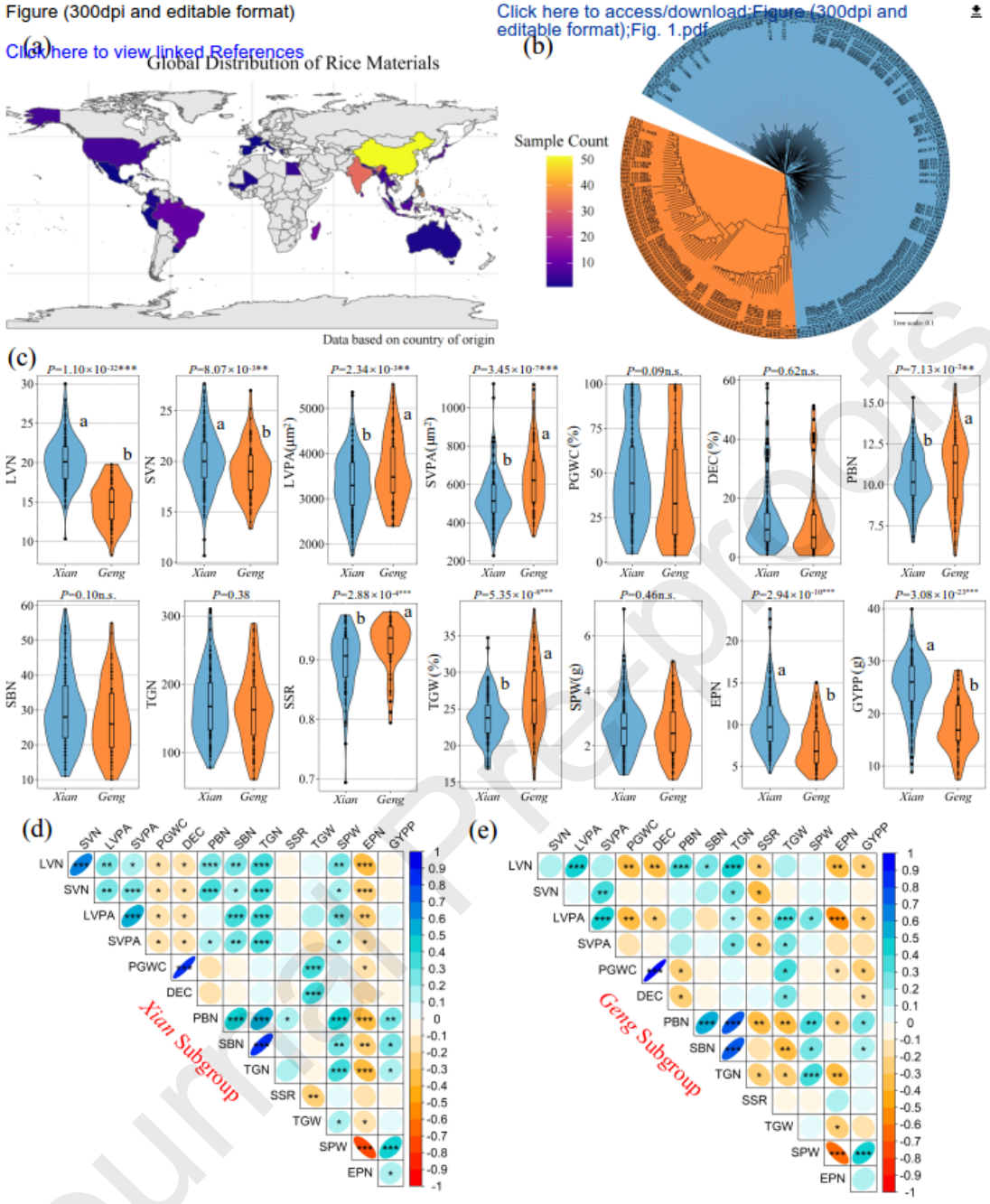

Figure (300dpi and editable format)

Click here to view linked References

Click here to access/download;Figure (300dpi and editable format);Fig. 2.pdf

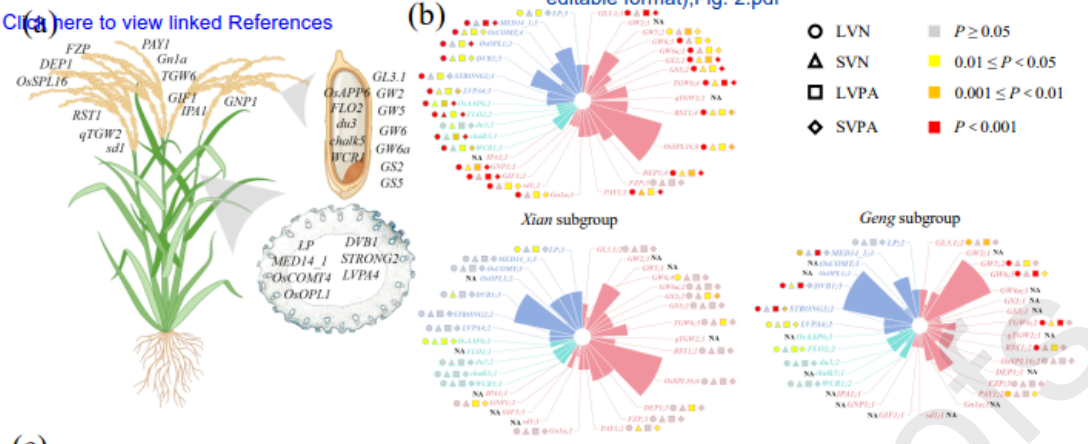

(c)

Groups	*Geng* subgroup											*Xian* subgroup								
Genes	*LVPA4*	*FLO2*	*STRONG2*	*GL3.1*	*GW5*	*GW6*	*TGW6*	*DVB1*	*MED14_1*	*RST1*	*PAY1*	*OsAAP6*	*GW6*	*LP*	*PAY1*	*DVB1*	*GS2*	*GNP1*	*TGW6*	*DEP1*
Haplotypes Variation	Hap3→2	Hap2→1	Hap3→1	Hap2→3	Hap1→2	Hap5→3	Hap4→2	Hap3→2	Hap4→2	Hap2→3	Hap2→3	Hap1→2	Hap4→3	Hap2→3	Hap3→1	Hap1→4	Hap1→2	Hap2→1	Hap3→1	Hap4→3
LVN	+	+	+	+	+	+	+	+	+	+	+	+	+	+	0	0	0	0	0	0
SVN	+	0	0	0	0	0	0	0	0	0	0	+	0	0	+	+	0	0	0	0
LVPA (μm²)	+	+	+	+	+	+	+	+	+	+	0	+	0	+	0	0	+	+	+	+
SVPA (μm²)	+	+	+	0	0	0	0	0	0	0	-	+	0	0	+	0	+	+	0	0
PGWC (%)	-	-	0	-	-	0	0	0	0	-	+	0	0	0	0	0	+	0	-	-
DEC (%)	-	-	0	-	-	0	0	0	0	-	+	0	0	0	0	0	+	0	-	-
TGW (g)	0	+	0	0	0	0	+	+	+	0	-	0	0	0	0	+	0	+	-	0
PBN	+	+	+	+	+	+	+	+	+	+	+	0	0	0	0	0	0	0	0	0
SBN	+	0	0	0	0	0	0	0	0	0	0	0	0	+	+	0	0	0	+	0
TGN	+	+	+	+	+	+	+	+	+	+	+	0	0	+	+	0	+	0	+	0
SSR	0	0	0	0	0	0	0	0	0	0	0	0	0	0	0	0	0	0	0	0
SPW (g)	+	+	+	+	+	+	+	+	+	+	0	0	0	+	0	+	+	0	0	0
EPN	-	-	-	-	-	-	-	-	-	0	0	0	0	-	0	-	-	-	0	0
GYPP (g)	0	0	0	0	0	-	-	-	-	+	0	0	0	0	0	0	0	0	0	0

Figure (300dpi and editable format)

Click here to access/download;Figure (300dpi and editable format);Fig. 3.pdf

Click here to view linked References

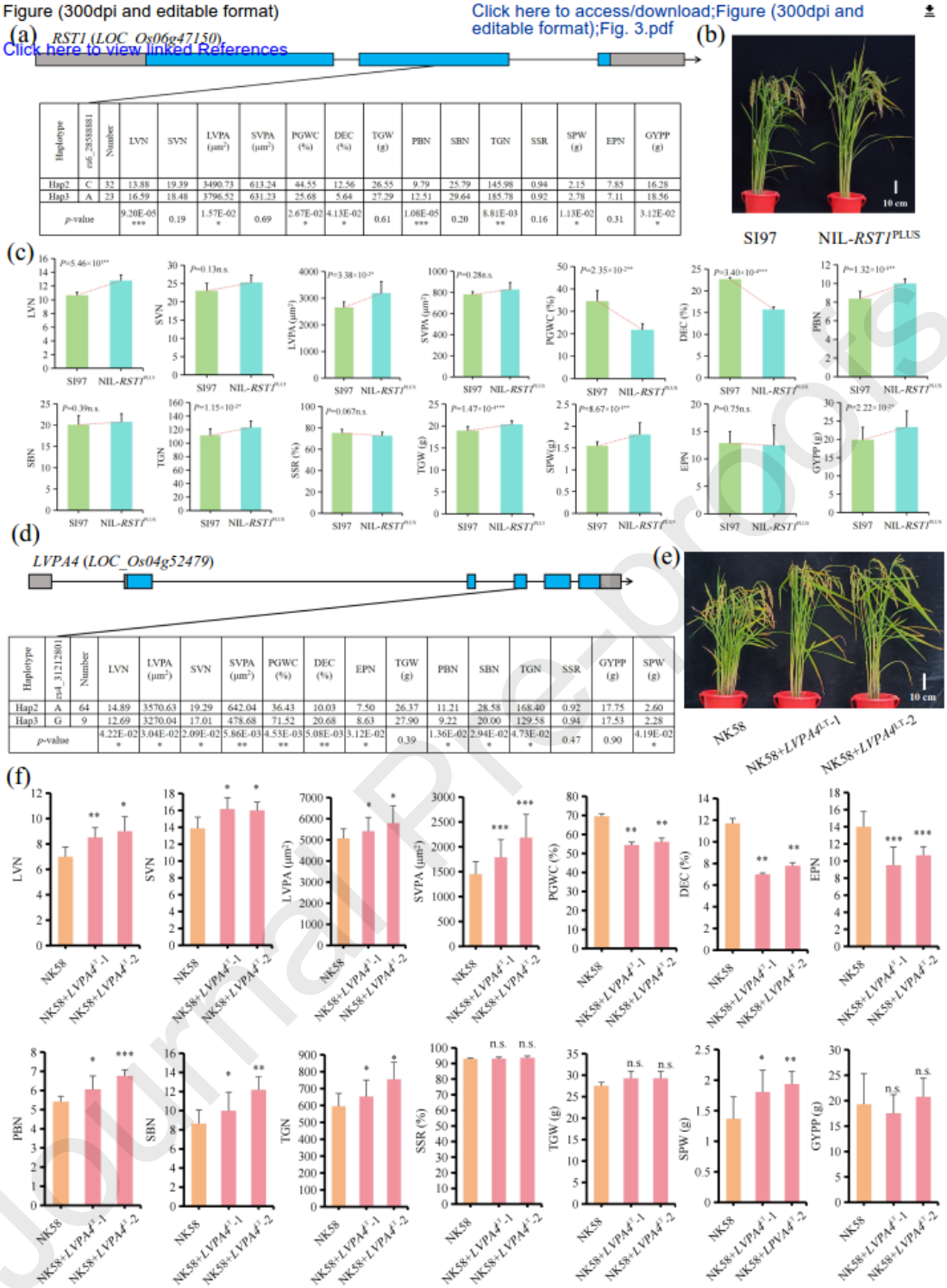

Haplotype	rs6_28588881	Number	LVN	SVN	LVPA (μm²)	SVPA (μm²)	PGWC (%)	DEC (%)	TGW (g)	PBN	SBN	TGN	SSR	SPW (g)	EPN	GYPP (g)
Hap2	C	32	13.88	19.39	3490.73	613.24	44.55	12.56	26.55	9.79	25.79	145.98	0.94	2.15	7.85	16.28
Hap3	A	23	16.59	18.48	3796.52	631.23	25.68	5.64	27.29	12.51	29.64	185.78	0.92	2.78	7.11	18.56
p-value			9.20E-05 ***	0.19	1.57E-02 *	0.69	2.67E-02 *	4.13E-02 *	0.61	1.08E-05 ***	0.20	8.81E-03 **	0.16	1.13E-02 *	0.31	3.12E-02 *

Haplotype	ps4_31212801	Number	LVN	LVPA (μm²)	SVN	SVPA (μm²)	PGWC (%)	DEC (%)	EPN	TGW (g)	PBN	SBN	TGN	SSR	GYPP (g)	SPW (g)
Hap2	A	64	14.89	3570.63	19.29	642.04	36.43	10.03	7.50	26.37	11.21	28.58	168.40	0.92	17.75	2.60
Hap3	G	9	12.69	3270.04	17.01	478.68	71.52	20.68	8.63	27.90	9.22	20.00	129.58	0.94	17.53	2.28
p-value			4.22E-02 *	3.04E-02 *	2.09E-02 *	5.86E-03 **	4.53E-03 **	5.08E-03 **	3.12E-02 *	0.39	1.36E-02 *	2.94E-02 *	4.73E-02 *	0.47	0.90	4.19E-02 *

Figure (300dpi and editable format)

Click here to access/download;Figure (300dpi and editable format);Fig. 4.pdf

Click here to view linked References

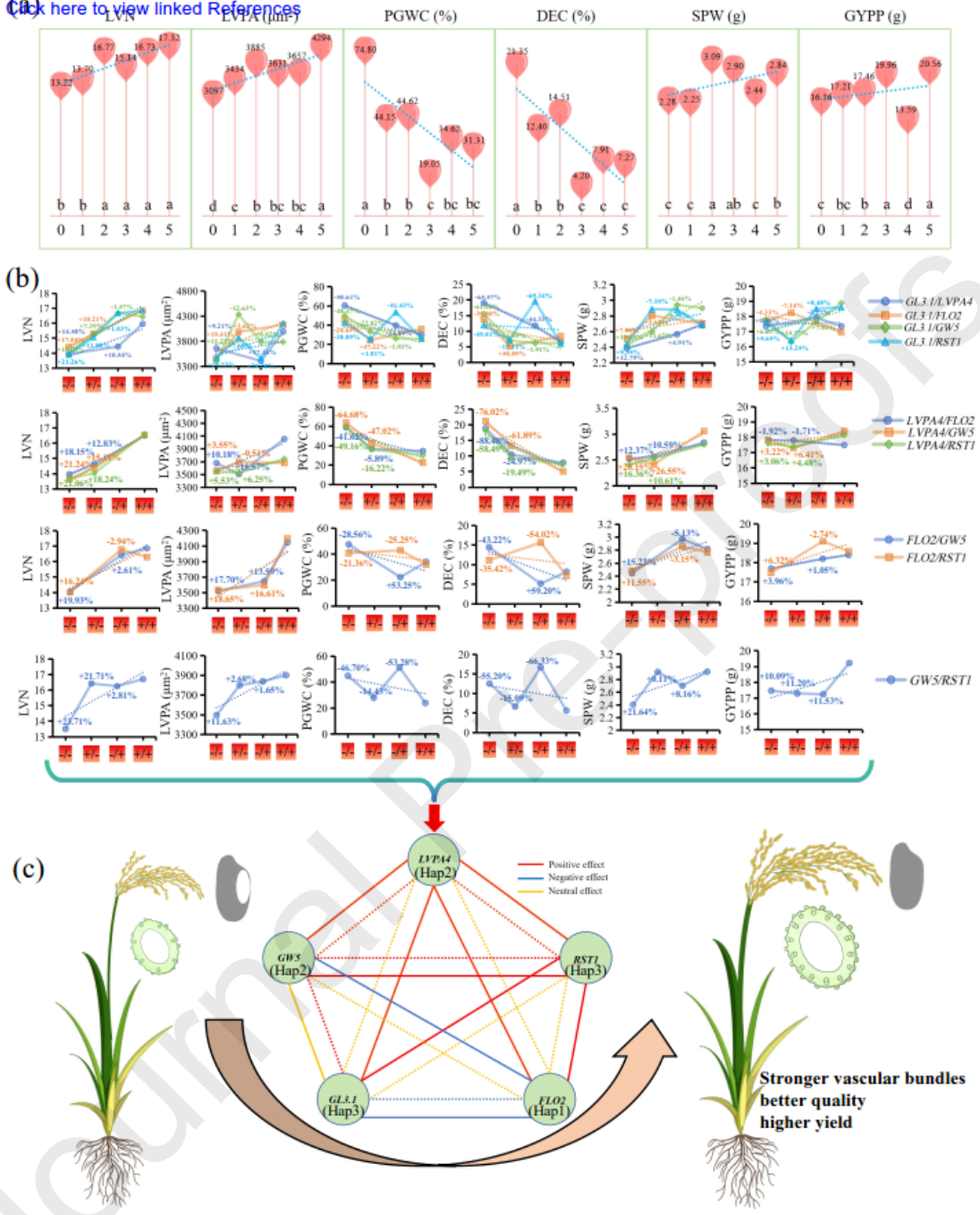

Figure (300dpi and editable format)

Click here to access/download;Figure (300dpi and editable format);Fig. 5.pdf

Click here to view linked References

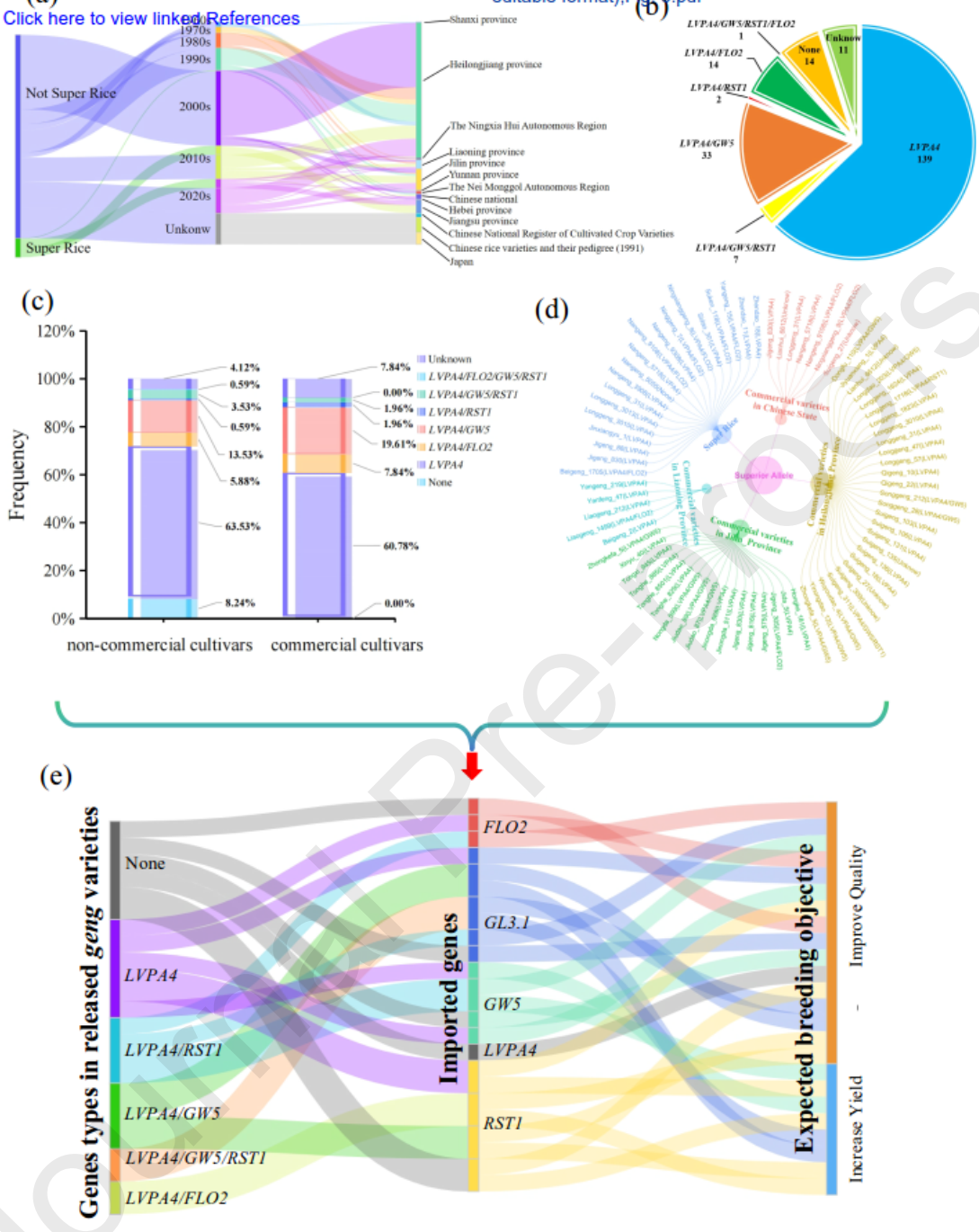

Figure (300dpi and editable format)

Click here to view linked References

Click here to access/download;Figure (300dpi and editable format);Fig. 2.pdf

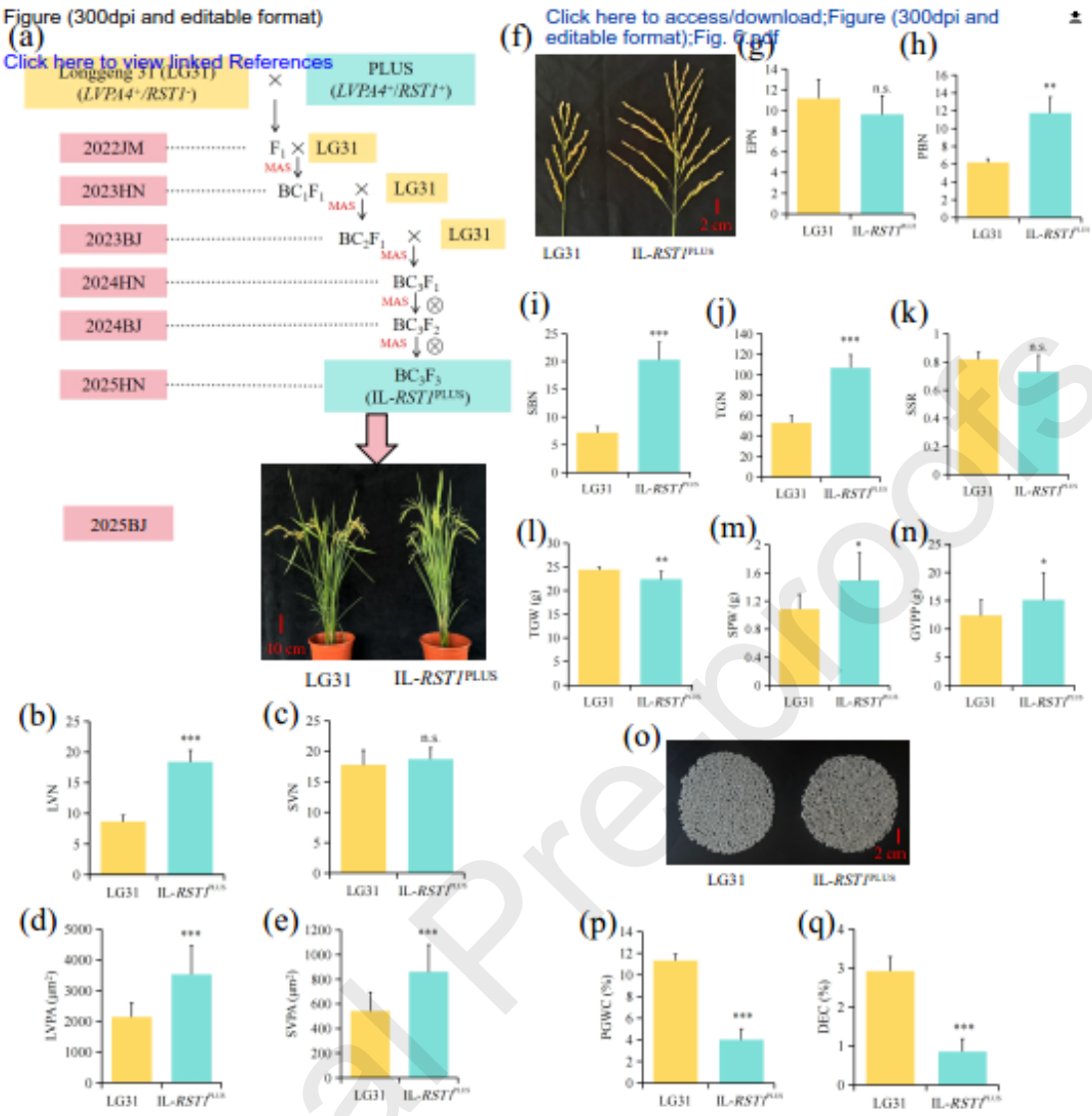

Figure (300dpi and editable format)

Click here to view linked References

Click here to access/download;Figure (300dpi and editable format);Fig. 7.pdf